

New physics in the angular distribution of $B_c^- \rightarrow J/\psi(\rightarrow \mu^+ \mu^-) \tau^- (\rightarrow \pi^- \nu_\tau) \bar{\nu}_\tau$ decay

Quan-Yi Hu,^a Xin-Qiang Li,^b Xiao-Long Mu,^b Ya-Dong Yang^b and Dong-Hui Zheng^b

^a*School of Physics and Electrical Engineering, Anyang Normal University, Anyang, Henan 455000, China*

^b*Institute of Particle Physics and Key Laboratory of Quark and Lepton Physics (MOE), Central China Normal University, Wuhan, Hubei 430079, China*

E-mail: qyhu@aynu.edu.cn

ABSTRACT: In $B_c^- \rightarrow J/\psi(\rightarrow \mu^+ \mu^-) \tau^- \bar{\nu}_\tau$ decay, the three-momentum \mathbf{p}_{τ^-} cannot be determined accurately due to the decay products of τ^- inevitably include an undetected ν_τ . As a consequence, the angular distribution of this decay cannot be measured. In this work, we construct a *measurable* angular distribution by considering the subsequent decay $\tau^- \rightarrow \pi^- \nu_\tau$. The full cascade decay is $B_c^- \rightarrow J/\psi(\rightarrow \mu^+ \mu^-) \tau^- (\rightarrow \pi^- \nu_\tau) \bar{\nu}_\tau$, in which the three-momenta \mathbf{p}_{μ^+} , \mathbf{p}_{μ^-} , and \mathbf{p}_{π^-} can be measured. The five-fold differential angular distribution containing all Lorentz structures of the new physics (NP) effective operators can be written in terms of twelve angular observables $\mathcal{I}_i(q^2, E_\pi)$. Integrating over the energy of pion E_π , we construct twelve normalized angular observables $\widehat{\mathcal{I}}_i(q^2)$ and two lepton-flavor-universality ratios $R(P_{L,T}^{J/\psi})(q^2)$. Based on the $B_c \rightarrow J/\psi$ form factors calculated by the latest lattice QCD and sum rule, we predict the q^2 distribution of all $\widehat{\mathcal{I}}_i$ and $R(P_{L,T}^{J/\psi})$ both within the Standard Model and in eight NP benchmark points. We find that the benchmark BP2 (corresponding to the hypothesis of tensor operator) has the greatest effect on all $\widehat{\mathcal{I}}_i$ and $R(P_{L,T}^{J/\psi})$, except $\widehat{\mathcal{I}}_5$. The ratios $R(P_{L,T}^{J/\psi})$ are more sensitive to the NP with pseudo-scalar operators than the $\widehat{\mathcal{I}}_i$. Finally, we discuss the symmetries in the angular observables and present a model-independent method to determine the existence of tensor operators.

Contents

1	Introduction	1
2	Analytical results	3
2.1	Effective Hamiltonian	3
2.2	Transversity amplitudes	3
2.3	Angular distribution	5
3	Integrated observables	6
4	Numerical results	8
4.1	The form factors	8
4.2	The NP benchmark points	8
4.3	Angular observables $\widehat{\mathcal{L}}_i(q^2)$	9
4.4	Lepton-flavor-universality ratios $R(P_{L,T}^{J/\psi})(q^2)$ and $R(J/\psi)$	11
5	Symmetries in the angular observables without tensor operators	12
6	Conclusions	14
A	The calculation of the angular distribution	15
A.1	Definitions and conventions	15
A.2	Calculating $J/\psi \rightarrow \mu^+ \mu^-$ decay	17
A.3	Dimensionless factors	17
B	The detailed derivation of the dependence relations	18

1 Introduction

Exploring new physics (NP) beyond the Standard Model (SM) has been one of the most important tasks in high energy physics, especially since the discovery of Higgs boson [1–3]. In recent years, the existence of NP that breaks the universality of lepton flavour in $b \rightarrow c\tau^- \bar{\nu}_\tau$ transition has been implied by the anomalous measurements [4–12] on $\bar{B} \rightarrow D^{(*)}\tau^- \bar{\nu}_\tau$ decays. Moreover, the averaging results performed by the Heavy Flavor Averaging Group (HFLAV) [13] show that the measurements of $R(D^{(*)}) \equiv \mathcal{B}(\bar{B} \rightarrow D^{(*)}\tau\bar{\nu})/\mathcal{B}(\bar{B} \rightarrow D^{(*)}\ell\bar{\nu})$ ($\ell = e, \mu$) deviate about 3.1σ [14] from the predicted values within the SM.¹ Motivated by this deviation and using the available data on $b \rightarrow c\tau^- \bar{\nu}_\tau$ transition, a number of global fitting analyses have been carried out [16–23], finding that some different combinations of

¹The recent ref. [15] finds $R(D^*) = 0.250 \pm 0.003$ in the SM. Since the HFLAV average don't include this value, the actual deviation from the SM prediction is larger than 3.1σ .

NP coupling parameters can well explain the $R(D^{(*)})$ anomaly. At the same time, a large number of works have been completed in some specific NP models, such as leptoquarks [24–34], R -parity violating supersymmetric models [35–39], charged Higgses [24, 40–43], charged vector bosons [44–46], and Pati-Salam Model [47]. These NP effects also affect other $b \rightarrow c$ semileptonic decay modes, such as $B_c \rightarrow J/\psi\tau\bar{\nu}_\tau$ [48–61], $B_c \rightarrow \eta_c\tau\bar{\nu}_\tau$ [52–54, 58–63], $\Lambda_b \rightarrow \Lambda_c\tau\bar{\nu}_\tau$ [17, 64–74], $\Xi_b \rightarrow \Xi_c\tau\bar{\nu}_\tau$ [75–78], $\Sigma_b \rightarrow \Sigma_c\tau\bar{\nu}_\tau$ [79, 80], and $\Omega_b \rightarrow \Omega_c\tau\bar{\nu}_\tau$ [79, 80].

Particularly, the LHCb collaboration released a value of the ratio $R(J/\psi) \equiv \mathcal{B}(B_c \rightarrow J/\psi\tau\nu)/\mathcal{B}(B_c \rightarrow J/\psi\mu\nu) = 0.71 \pm 0.17 \pm 0.18$ [48]. Using the model-dependent calculations of $B_c \rightarrow J/\psi$ transition form factors [51, 53, 54, 59, 60, 81–90], the SM prediction of $R(J/\psi)$ lies in the range 0.23–0.30. The model-independent bound on $R(J/\psi)$ [56, 58] is also obtained by constraining the $B_c \rightarrow J/\psi$ form factors through a combination of dispersive relations, heavy-quark relations at zero-recoil, and the limited existing form-factor determinations from lattice QCD [91, 92], resulting in $0.20 \leq R(J/\psi) \leq 0.39$ [56]. Very recently, the HPQCD collaboration present the first lattice QCD determination of the vector and axial-vector form factors of the $B_c \rightarrow J/\psi$ transition for the full q^2 range [50], and find $R(J/\psi) = 0.2582 \pm 0.0038$ [49] within the SM, which is the most accurate prediction and in tension with the LHCb result at 1.8σ level. The $B_c \rightarrow J/\psi$ transition form factors from lattice QCD make the theoretical calculations more accurate, which makes it interesting to revisit the NP effects in $B_c \rightarrow J/\psi\tau\bar{\nu}_\tau$ decay.

In order to distinguish between the SM and NP scenarios, and further characterise the underlying effects of NP, besides considering the total decay rate, the full angular distribution of $B_c^- \rightarrow J/\psi\tau^-\bar{\nu}_\tau$ and $B_c^- \rightarrow J/\psi(\rightarrow \mu^+\mu^-)\tau^-\bar{\nu}_\tau$ decays should also be taken into account sometimes, see for instance refs. [49, 55, 59]. However, as pointed out by refs. [74, 93], the information of the polar and azimuthal angles of the emitted τ^- cannot be determined precisely because the decay products of τ^- inevitably contain an undetected ν_τ . This means that the “observables” depending on the polar or azimuthal angle of τ^- , such as the forward-backward asymmetry of τ^- and the convexity parameter, are unmeasurable theoretically and cannot be regarded as real observables. Therefore, in this work, we construct a *measurable* angular distribution by further considering the subsequent decay $\tau^- \rightarrow \pi^-\nu_\tau$. The full cascade decay is $B_c^- \rightarrow J/\psi(\rightarrow \mu^+\mu^-)\tau^-(\rightarrow \pi^-\nu_\tau)\bar{\nu}_\tau$, which includes three visible final-state particles μ^+ , μ^- , and π^- whose three-momenta can be measured. We first calculate the full five-fold differential angular distribution including all Lorentz structures of the NP effective operators, and then carefully study the NP effects in the angular distribution from many aspects.

Our paper is organized as follows. In section 2, after defining the effective Hamiltonian, we give the analytical results of the independent transversity amplitudes and the measurable angular distribution of the five-body $B_c^- \rightarrow J/\psi(\rightarrow \mu^+\mu^-)\tau^-(\rightarrow \pi^-\nu_\tau)\bar{\nu}_\tau$ decay. Definitions of the integrated observables are included in section 3. In section 4, we show the numerical results of the entire set of normalized angular observables $\widehat{\mathcal{L}}_i(q^2)$ and the lepton-flavor-universality ratios $R(P_{L,T}^{J/\psi})(q^2)$ and $R(J/\psi)$. A model-independent method for determining the existence of tensor operator is given in section 5. Our conclusions are finally made in section 6. In the appendices A and B, we present the detailed procedures related to the calculations of angular distribution and dependence relations, respectively.

2 Analytical results

In this section, after giving some necessary definitions, we directly list the analytical results of angular distribution. The more detailed calculations, including some useful conventions, can be found in appendix A.

2.1 Effective Hamiltonian

Assuming that the NP scale is higher than the electroweak scale, one can integrate out the possible NP particles as well as the SM heavy particles — the W^\pm , Z^0 , the top quark, and the Higgs boson, thus obtaining the effective Hamiltonian suitable for describing the $b \rightarrow c\tau^-\bar{\nu}_\tau$ transition²

$$\begin{aligned} \mathcal{H}_{\text{eff}} = & \sqrt{2}G_F V_{cb} [g_V(\bar{c}\gamma^\mu b)(\bar{\tau}\gamma_\mu\nu_{\tau L}) + g_A(\bar{c}\gamma^\mu\gamma_5 b)(\bar{\tau}\gamma_\mu\nu_{\tau L}) \\ & + g_S(\bar{c}b)(\bar{\tau}\nu_{\tau L}) + g_P(\bar{c}\gamma_5 b)(\bar{\tau}\nu_{\tau L}) \\ & + g_T(\bar{c}\sigma^{\mu\nu}(1 - \gamma_5)b)(\bar{\tau}\sigma_{\mu\nu}\nu_{\tau L})] + \text{H.c.}, \end{aligned} \quad (2.1)$$

where G_F is the Fermi constant, V_{cb} is the CKM matrix element, $\sigma^{\mu\nu} \equiv \frac{i}{2}[\gamma^\mu, \gamma^\nu]$, and $\nu_{\tau L} = P_L\nu_\tau$ denotes the field of left-handed neutrino. The NP effects are encoded in the Wilson coefficients g_i , which are defined at the typical energy scale $\mu = m_b$. In the SM, $g_V = -g_A = 1$ and $g_S = g_P = g_T = 0$.

2.2 Transversity amplitudes

In the calculation, the hadronic matrix elements contain the nonperturbative QCD effects and can be parameterized as the Lorentz invariant form factors. The vector and axial-vector current matrix elements can be written as the following four form factors [25, 50, 97]

$$\begin{aligned} \langle J/\psi(k, \varepsilon) | \bar{c}\gamma_\mu b | B_c(p) \rangle &= \frac{2iV(q^2)}{m_{B_c} + m_{J/\psi}} \epsilon_{\mu\nu\alpha\beta} \varepsilon^{*\nu} k^\alpha p^\beta, \quad (2.2) \\ \langle J/\psi(k, \varepsilon) | \bar{c}\gamma_\mu\gamma_5 b | B_c(p) \rangle &= 2m_{J/\psi} A_0(q^2) \frac{\varepsilon^* \cdot q}{q^2} q_\mu \\ &+ (m_{B_c} + m_{J/\psi}) A_1(q^2) \left(\varepsilon_\mu^* - \frac{\varepsilon^* \cdot q}{q^2} q_\mu \right) \\ &- A_2(q^2) \frac{\varepsilon^* \cdot q}{m_{B_c} + m_{J/\psi}} \left(p_\mu + k_\mu - \frac{m_{B_c}^2 - m_{J/\psi}^2}{q^2} q_\mu \right), \quad (2.3) \end{aligned}$$

where $q = p - k$, ε^μ denotes the polarization vector of J/ψ meson. In our numerical analysis, we will use the vector and axial-vector form factors computed in lattice QCD [49, 50].

Using the equation of motion, the scalar and pseudo-scalar matrix elements can be obtained by

$$\langle J/\psi(k, \varepsilon) | \bar{c}b | B_c(p) \rangle = 0, \quad (2.4)$$

²Neutrinos are assumed to be left-handed in this work. The effective Hamiltonian containing right-handed neutrinos can be found in refs. [94–96]. It can be derived from the identity $\sigma^{\mu\nu}\gamma_5 = -\frac{i}{2}\epsilon^{\mu\nu\alpha\beta}\sigma_{\alpha\beta}$ that the operator $(\bar{c}\sigma^{\mu\nu}(1 + \gamma_5)b)(\bar{\tau}\sigma_{\mu\nu}\nu_{\tau L})$ is absent. We use the convention $\epsilon_{0123} = -\epsilon^{0123} = 1$.

$$\langle J/\psi(k, \varepsilon) | \bar{c} \gamma_5 b | B_c(p) \rangle = -\varepsilon^* \cdot q \frac{2m_{J/\psi}}{m_b + m_c} A_0(q^2), \quad (2.5)$$

Based on the above four form factors $V(q^2)$ and $A_{0,1,2}(q^2)$, one can define four independent transversity amplitudes as follows

$$\mathcal{A}_t = \mathcal{A}_t^{SP} + \frac{m_\tau}{\sqrt{q^2}} \mathcal{A}_t^{VA}, \quad (2.6)$$

$$\mathcal{A}_0 = g_A \frac{m_{B_c} + m_{J/\psi}}{2m_{J/\psi} \sqrt{q^2}} \left[A_1(q^2)(m_{B_c}^2 - m_{J/\psi}^2 - q^2) - A_2(q^2) \frac{Q_+ Q_-}{(m_{B_c} + m_{J/\psi})^2} \right], \quad (2.7)$$

$$\mathcal{A}_\perp = g_A \sqrt{2} A_1(q^2) (m_{B_c} + m_{J/\psi}), \quad (2.8)$$

$$\mathcal{A}_\parallel = g_V \sqrt{2} V(q^2) \frac{\sqrt{Q_+ Q_-}}{m_{B_c} + m_{J/\psi}}, \quad (2.9)$$

with

$$\mathcal{A}_t^{SP} = -g_P A_0(q^2) \frac{\sqrt{Q_+ Q_-}}{m_b + m_c}, \quad \mathcal{A}_t^{VA} = g_A A_0(q^2) \frac{\sqrt{Q_+ Q_-}}{\sqrt{q^2}}, \quad (2.10)$$

where m_b and m_c are the current quark masses evaluated at the scale $\mu = m_b$, and $Q_\pm \equiv (m_{B_c} \pm m_{J/\psi})^2 - q^2$.

The tensor matrix element can be parameterized as [25, 59, 97]

$$\begin{aligned} \langle J/\psi(k, \varepsilon) | \bar{c} \sigma_{\mu\nu} b | B_c(p) \rangle = & \epsilon_{\mu\nu\alpha\beta} \left\{ -\varepsilon^{*\alpha} (k+p)^\beta T_1(q^2) \right. \\ & + \frac{m_{B_c}^2 - m_{J/\psi}^2}{q^2} \varepsilon^{*\alpha} q^\beta [T_1(q^2) - T_2(q^2)] \\ & \left. + 2 \frac{\varepsilon^* \cdot q}{q^2} p^\alpha k^\beta \left[T_1(q^2) - T_2(q^2) - \frac{q^2}{m_{B_c}^2 - m_{J/\psi}^2} T_3(q^2) \right] \right\}, \end{aligned} \quad (2.11)$$

and $\langle J/\psi | \bar{c} \sigma_{\mu\nu} \gamma_5 b | B_c \rangle = -\frac{i}{2} \epsilon_{\mu\nu\alpha\beta} \langle J/\psi | \bar{c} \sigma^{\alpha\beta} b | B_c \rangle$. In the presence of the tensor operators, we find three additional independent transversity amplitudes as follows

$$\mathcal{A}_0^T = g_T \frac{1}{2m_{J/\psi}} \left[T_2(q^2)(m_{B_c}^2 + 3m_{J/\psi}^2 - q^2) - T_3(q^2) \frac{Q_+ Q_-}{m_{B_c}^2 - m_{J/\psi}^2} \right], \quad (2.12)$$

$$\mathcal{A}_\perp^T = g_T \sqrt{2} T_2(q^2) \frac{m_{B_c}^2 - m_{J/\psi}^2}{\sqrt{q^2}}, \quad (2.13)$$

$$\mathcal{A}_\parallel^T = g_T \sqrt{2} T_1(q^2) \frac{\sqrt{Q_+ Q_-}}{\sqrt{q^2}}, \quad (2.14)$$

here the superscript T indicates that an amplitude appears only when one consider the tensor operators.

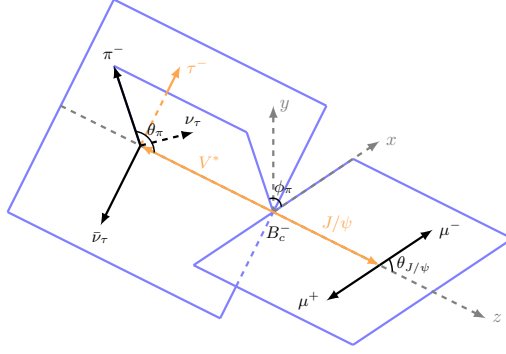


Figure 1. Definition of the angles in the $B_c^- \rightarrow J/\psi(\rightarrow \mu^+ \mu^-) \tau^- (\rightarrow \pi^- \nu_\tau) \bar{\nu}_\tau$ decay.

2.3 Angular distribution

The *measurable* angular distribution of the five-body $B_c^- \rightarrow J/\psi(\rightarrow \mu^+ \mu^-) \tau^- (\rightarrow \pi^- \nu_\tau) \bar{\nu}_\tau$ decay can be written as

$$\frac{d^5\Gamma}{dq^2 dE_\pi d\cos\theta_\pi d\phi_\pi d\cos\theta_{J/\psi}} = \frac{3G_F^2 |V_{cb}|^2 |\mathbf{p}_{J/\psi}| (q^2)^{3/2} m_\tau^2}{256\pi^4 m_{B_c}^2 (m_\tau^2 - m_\pi^2)^2} \mathcal{B}_\tau \mathcal{B}_{J/\psi} \times \mathcal{I}(q^2, E_\pi, \cos\theta_{J/\psi}, \cos\theta_\pi, \phi_\pi), \quad (2.15)$$

where $|\mathbf{p}_{J/\psi}| = \sqrt{Q_+ Q_-}/(2m_{B_c})$ denotes the magnitude of three-momentum of the J/ψ meson in the B_c rest frame. $\mathcal{B}_\tau \equiv \mathcal{B}(\tau \rightarrow \pi^- \nu_\tau)$ and $\mathcal{B}_{J/\psi} \equiv \mathcal{B}(J/\psi \rightarrow \mu^- \mu^+)$ are the branching fractions of $\tau \rightarrow \pi^- \nu_\tau$ and $J/\psi \rightarrow \mu^- \mu^+$ decays, respectively. q^2 is invariant mass squared of the $\tau^- \bar{\nu}_\tau$; $\theta_{J/\psi}$ denotes the polar angle of μ^- in the J/ψ rest frame; E_π , θ_π , and ϕ_π represent the energy, polar angle, and azimuthal angle of π^- in the $\tau^- \bar{\nu}_\tau$ center-of-mass frame, respectively. A more intuitive definition of the angles is shown in figure 1. The function $\mathcal{I}(q^2, E_\pi, \cos\theta_{J/\psi}, \cos\theta_\pi, \phi_\pi)$ can be decomposed into a set of trigonometric functions as follows

$$\begin{aligned} \mathcal{I}(q^2, E_\pi, \cos\theta_{J/\psi}, \cos\theta_\pi, \phi_\pi) &= \sum_{i=1}^{12} \mathcal{I}_i(q^2, E_\pi) \Omega_i(\cos\theta_{J/\psi}, \cos\theta_\pi, \phi_\pi) \\ &\equiv \mathcal{I}_{1c} \cos^2\theta_{J/\psi} + \mathcal{I}_{1s} \sin^2\theta_{J/\psi} \\ &\quad + (\mathcal{I}_{2c} \cos^2\theta_{J/\psi} + \mathcal{I}_{2s} \sin^2\theta_{J/\psi}) \cos 2\theta_\pi \\ &\quad + (\mathcal{I}_{6c} \cos^2\theta_{J/\psi} + \mathcal{I}_{6s} \sin^2\theta_{J/\psi}) \cos\theta_\pi \\ &\quad + (\mathcal{I}_3 \cos 2\phi_\pi + \mathcal{I}_9 \sin 2\phi_\pi) \sin^2\theta_\pi \sin^2\theta_{J/\psi} \\ &\quad + (\mathcal{I}_4 \cos\phi_\pi + \mathcal{I}_8 \sin\phi_\pi) \sin 2\theta_\pi \sin 2\theta_{J/\psi} \\ &\quad + (\mathcal{I}_5 \cos\phi_\pi + \mathcal{I}_7 \sin\phi_\pi) \sin\theta_\pi \sin 2\theta_{J/\psi}. \end{aligned} \quad (2.16)$$

The twelve angular observables $\mathcal{I}_i(q^2, E_\pi)$ can be completely expressed in terms of the seven transversity amplitudes defined in subsection 2.2 and the dimensionless factors listed in appendix A.3.

$$\mathcal{I}_{1c} = S_1 |\mathcal{A}_\perp|^2 - 2R_1 \text{Re}[\mathcal{A}_\perp \mathcal{A}_\perp^{T*}] + 4S_1^T |\mathcal{A}_\perp^T|^2 + (\perp \leftrightarrow \parallel), \quad (2.17)$$

$$\begin{aligned} \mathcal{I}_{1s} = & S_t |\mathcal{A}_t|^2 + (S_1 - S_3) |\mathcal{A}_0|^2 - 2(R_1 - R_3) \text{Re} [\mathcal{A}_0 \mathcal{A}_0^{T*}] + 4(S_1^T - S_3^T) |\mathcal{A}_0^T|^2 \\ & + \frac{1}{2} \left\{ S_1 |\mathcal{A}_\perp|^2 - 2R_1 \text{Re} [\mathcal{A}_\perp \mathcal{A}_\perp^{T*}] + 4S_1^T |\mathcal{A}_\perp^T|^2 + (\perp \leftrightarrow \parallel) \right\}, \end{aligned} \quad (2.18)$$

$$\mathcal{I}_{2c} = S_3 |\mathcal{A}_\perp|^2 - 2R_3 \text{Re} [\mathcal{A}_\perp \mathcal{A}_\perp^{T*}] + 4S_3^T |\mathcal{A}_\perp^T|^2 + (\perp \leftrightarrow \parallel), \quad (2.19)$$

$$\begin{aligned} \mathcal{I}_{2s} = & -2S_3 |\mathcal{A}_0|^2 + 4R_3 \text{Re} [\mathcal{A}_0 \mathcal{A}_0^{T*}] - 8S_3^T |\mathcal{A}_0^T|^2 \\ & + \frac{1}{2} \left\{ S_3 |\mathcal{A}_\perp|^2 - 2R_3 \text{Re} [\mathcal{A}_\perp \mathcal{A}_\perp^{T*}] + 4S_3^T |\mathcal{A}_\perp^T|^2 + (\perp \leftrightarrow \parallel) \right\}, \end{aligned} \quad (2.20)$$

$$\mathcal{I}_{6c} = 2\text{Re} \left[S_2 \mathcal{A}_\parallel \mathcal{A}_\perp^* - R_2 \left(\mathcal{A}_\perp \mathcal{A}_\parallel^{T*} + \mathcal{A}_\parallel \mathcal{A}_\perp^{T*} \right) + 4S_2^T \mathcal{A}_\parallel^T \mathcal{A}_\perp^{T*} \right], \quad (2.21)$$

$$\begin{aligned} \mathcal{I}_{6s} = & \text{Re} \left[S_2 \mathcal{A}_\parallel \mathcal{A}_\perp^* - R_2 \left(\mathcal{A}_\perp \mathcal{A}_\parallel^{T*} + \mathcal{A}_\parallel \mathcal{A}_\perp^{T*} \right) + 4S_2^T \mathcal{A}_\parallel^T \mathcal{A}_\perp^{T*} \right. \\ & \left. - \sqrt{2} R_t \mathcal{A}_t \mathcal{A}_0^* + 2\sqrt{2} R_t^T \mathcal{A}_t \mathcal{A}_0^{T*} \right], \end{aligned} \quad (2.22)$$

$$\mathcal{I}_3 = S_3 |\mathcal{A}_\perp|^2 - 2R_3 \text{Re} [\mathcal{A}_\perp \mathcal{A}_\perp^{T*}] + 4S_3^T |\mathcal{A}_\perp^T|^2 - (\perp \leftrightarrow \parallel), \quad (2.23)$$

$$\mathcal{I}_9 = 2\text{Im} \left[S_3 \mathcal{A}_\parallel \mathcal{A}_\perp^* + R_3 \left(\mathcal{A}_\perp \mathcal{A}_\parallel^{T*} - \mathcal{A}_\parallel \mathcal{A}_\perp^{T*} \right) + 4S_3^T \mathcal{A}_\parallel^T \mathcal{A}_\perp^{T*} \right], \quad (2.24)$$

$$\mathcal{I}_4 = \sqrt{2} \text{Re} \left[S_3 \mathcal{A}_\perp \mathcal{A}_0^* - R_3 \left(\mathcal{A}_0 \mathcal{A}_\perp^{T*} + \mathcal{A}_\perp \mathcal{A}_0^{T*} \right) + 4S_3^T \mathcal{A}_0^T \mathcal{A}_\perp^{T*} \right], \quad (2.25)$$

$$\mathcal{I}_8 = \sqrt{2} \text{Im} \left[S_3 \mathcal{A}_\parallel \mathcal{A}_0^* + R_3 \left(\mathcal{A}_0 \mathcal{A}_\parallel^{T*} - \mathcal{A}_\parallel \mathcal{A}_0^{T*} \right) + 4S_3^T \mathcal{A}_\parallel^T \mathcal{A}_0^{T*} \right], \quad (2.26)$$

$$\begin{aligned} \mathcal{I}_5 = & \frac{1}{2\sqrt{2}} \text{Re} \left[2S_2 \mathcal{A}_\parallel \mathcal{A}_0^* - 2R_2 \left(\mathcal{A}_0 \mathcal{A}_\parallel^{T*} + \mathcal{A}_\parallel \mathcal{A}_0^{T*} \right) + 8S_2^T \mathcal{A}_\parallel^T \mathcal{A}_0^{T*} \right. \\ & \left. + \sqrt{2} R_t \mathcal{A}_t \mathcal{A}_\perp^* - 2\sqrt{2} R_t^T \mathcal{A}_t \mathcal{A}_\perp^{T*} \right], \end{aligned} \quad (2.27)$$

$$\begin{aligned} \mathcal{I}_7 = & \frac{1}{2\sqrt{2}} \text{Im} \left[2S_2 \mathcal{A}_\perp \mathcal{A}_0^* + 2R_2 \left(\mathcal{A}_0 \mathcal{A}_\perp^{T*} - \mathcal{A}_\perp \mathcal{A}_0^{T*} \right) - 8S_2^T \mathcal{A}_0^T \mathcal{A}_\perp^{T*} \right. \\ & \left. - \sqrt{2} R_t \mathcal{A}_t \mathcal{A}_\parallel^* + 2\sqrt{2} R_t^T \mathcal{A}_t \mathcal{A}_\parallel^{T*} \right]. \end{aligned} \quad (2.28)$$

In the SM, the angular observables \mathcal{I}_7 , \mathcal{I}_8 , and \mathcal{I}_9 are vanishing. Therefore, in future measurements, a non-vanishing \mathcal{I}_7 , \mathcal{I}_8 , or \mathcal{I}_9 would be a solid signal of NP, which induces a complex contribution to the amplitude.

3 Integrated observables

The differential decay rate (2.15) depends on five parameters q^2 , E_π , $\theta_{J/\psi}$, θ_π and ϕ_π , and a complete experimental analysis may be limited by statistics. Integrating over the E_π and after proper normalization, we can get the following angular function

$$\begin{aligned} \widehat{\mathcal{I}}(q^2, \cos \theta_{J/\psi}, \cos \theta_\pi, \phi_\pi) & \equiv \frac{\int \frac{d^5 \Gamma}{dq^2 dE_\pi d \cos \theta_\pi d \phi_\pi d \cos \theta_{J/\psi}} dE_\pi}{\frac{d\Gamma}{dq^2}} \\ & = \frac{9}{8\pi} \sum_{i=1}^{12} \widehat{\mathcal{I}}_i(q^2) \Omega_i(\cos \theta_{J/\psi}, \cos \theta_\pi, \phi_\pi), \end{aligned} \quad (3.1)$$

with the twelve normalized angular observables $\widehat{\mathcal{I}}_i(q^2)$ defined as

$$\widehat{\mathcal{I}}_i(q^2) \equiv \frac{\int \mathcal{I}_i(q^2, E_\pi) dE_\pi}{\int (3\mathcal{I}_{1c} - \mathcal{I}_{2c} + 6\mathcal{I}_{1s} - 2\mathcal{I}_{2s}) dE_\pi}. \quad (3.2)$$

Our choice of the normalization in eq. (3.1) results the relationship $3\widehat{\mathcal{I}}_{1c}(q^2) - \widehat{\mathcal{I}}_{2c}(q^2) + 6\widehat{\mathcal{I}}_{1s}(q^2) - 2\widehat{\mathcal{I}}_{2s}(q^2) = 1$. The cancellations through normalization to the decay rate lead to the observables $\widehat{\mathcal{I}}_i(q^2)$ have less theoretical uncertainty to facilitate the discussion of the NP effects. In section 4, we will numerically analyse the entire set of observables $\widehat{\mathcal{I}}_i(q^2)$ within the SM and in some NP benchmark points.

The forward-backward asymmetry of π^- meson as a function of q^2 can be defined as

$$\begin{aligned} A_{FB}(q^2) &\equiv \frac{\int_0^1 \frac{d^2\Gamma}{dq^2 d\cos\theta_\pi} d\cos\theta_\pi - \int_{-1}^0 \frac{d^2\Gamma}{dq^2 d\cos\theta_\pi} d\cos\theta_\pi}{\frac{d\Gamma}{dq^2}} \\ &= \frac{3}{2} (\widehat{\mathcal{I}}_{6c} + 2\widehat{\mathcal{I}}_{6s}). \end{aligned} \quad (3.3)$$

This asymmetry observable only exists in τ channel, and specifically for the $\tau^- \rightarrow \pi^- \nu_\tau$ decay. Obviously, it can be expressed linearly in terms of angular observables $\widehat{\mathcal{I}}_i(q^2)$.

By integrating over the lepton-side parameters E_π , θ_π , ϕ_π , we can obtain the two-fold differential decay rate as follows

$$\frac{d^2\Gamma}{dq^2 d\cos\theta_{J/\psi}} = \frac{3}{8} \frac{d\Gamma}{dq^2} \left[2P_L^{J/\psi}(q^2) \sin^2\theta_{J/\psi} + P_T^{J/\psi}(q^2) (1 + \cos^2\theta_{J/\psi}) \right], \quad (3.4)$$

where

$$P_L^{J/\psi}(q^2) \equiv \frac{d\Gamma_L/dq^2}{d\Gamma_L/dq^2 + d\Gamma_T/dq^2}, \quad P_T^{J/\psi}(q^2) \equiv \frac{d\Gamma_T/dq^2}{d\Gamma_L/dq^2 + d\Gamma_T/dq^2}, \quad (3.5)$$

are the longitudinal and transverse polarization fractions of the J/ψ meson, respectively. The differential decay rates for the longitudinally and transversely polarized intermediate state J/ψ are given by

$$\begin{aligned} \frac{d\Gamma_L}{dq^2} &\equiv \frac{d\Gamma^{\lambda_{J/\psi}=0}}{dq^2} \\ &= \mathcal{N} \left\{ 3q^2 |\mathcal{A}_t|^2 + (m_\tau^2 + 2q^2) |\mathcal{A}_0|^2 \right. \\ &\quad \left. + 24m_\tau \sqrt{q^2} \text{Re} [\mathcal{A}_0 \mathcal{A}_0^{T*}] + 16 (2m_\tau^2 + q^2) |\mathcal{A}_0^T|^2 \right\}, \end{aligned} \quad (3.6)$$

$$\begin{aligned} \frac{d\Gamma_T}{dq^2} &\equiv \frac{d\Gamma^{\lambda_{J/\psi}=+1}}{dq^2} + \frac{d\Gamma^{\lambda_{J/\psi}=-1}}{dq^2} \\ &= \mathcal{N} \left\{ (m_\tau^2 + 2q^2) |\mathcal{A}_\perp|^2 + 24m_\tau \sqrt{q^2} \text{Re} [\mathcal{A}_\perp \mathcal{A}_\perp^{T*}] \right. \\ &\quad \left. + 16 (2m_\tau^2 + q^2) |\mathcal{A}_\perp^T|^2 + (\perp \leftrightarrow \parallel) \right\}, \end{aligned} \quad (3.7)$$

with the factor

$$\mathcal{N} \equiv \frac{G_F^2 |V_{cb}|^2 |\mathbf{p}_{J/\psi}|}{192\pi^3 m_{B_c}^2} \left(1 - \frac{m_\tau^2}{q^2}\right)^2 \mathcal{B}_\tau \mathcal{B}_{J/\psi}. \quad (3.8)$$

The polarization observables $P_{L,T}^{J/\psi}(q^2)$ constructed above are not affected by τ decay dynamics since we have integrated over all the lepton-side kinematic parameters, so they are also applicable to light leptons μ and e . We denote $\left[P_{L,T}^{J/\psi}\right]_\tau$ and $\left[P_{L,T}^{J/\psi}\right]_\mu$ as extraction from $B_c \rightarrow J/\psi\tau\nu$ and $B_c \rightarrow J/\psi\mu\nu$ decays respectively, and define the following ratios to probe the universality of lepton flavor

$$R\left(P_{L,T}^{J/\psi}\right) \equiv \frac{\left[P_{L,T}^{J/\psi}\right]_\tau}{\left[P_{L,T}^{J/\psi}\right]_\mu}. \quad (3.9)$$

The q^2 distribution of the decay rate can be obtained by adding up eqs. (3.6) and (3.7) as follows

$$\frac{d\Gamma}{dq^2} = \frac{d\Gamma_L}{dq^2} + \frac{d\Gamma_T}{dq^2}. \quad (3.10)$$

Our $d\Gamma/dq^2$ (apart from $\mathcal{B}_\tau \mathcal{B}_{J/\psi}$) is consistent with that in refs. [25, 49].

4 Numerical results

4.1 The form factors

The $B_c \rightarrow J/\psi$ transition form factors are the main source of theoretical uncertainties. For the $B_c \rightarrow J/\psi$ vector and axial-vector form factors, $V(q^2)$ and $A_{0,1,2}(q^2)$, we use the latest high-precision lattice QCD calculation results given in ref. [50]. Since the $B_c \rightarrow J/\psi$ tensor form factors $T_{1,2,3}(q^2)$ are not included in ref. [50], we will adopt the $T_{1,2,3}(q^2)$ calculated in the QCD sum rule method [59].³ These form factors are parameterized in a simplified z expansion to extend to the full q^2 range.

4.2 The NP benchmark points

The model-independent analyses of NP effects in $B \rightarrow D^{(*)}\tau\nu$ decays have been completed in many previous works [16–23]. In order to show the influences of these NP effects on the angular distribution of $B_c^- \rightarrow J/\psi(\rightarrow \mu^+\mu^-)\tau^- (\rightarrow \pi^-\nu_\tau)\bar{\nu}_\tau$ decay, we select various best-fit values as the NP benchmark points. These best-fit values are usually performed on a set of chiral base, which is equivalent to Eq. (2.1) by the following relations

$$\begin{aligned} g_V &= 1 + C_{V_L} + C_{V_R}, & g_A &= -1 - C_{V_L} + C_{V_R}, \\ g_S &= C_{S_L} + C_{S_R}, & g_P &= -C_{S_L} + C_{S_R}, & g_T &= C_T. \end{aligned} \quad (4.1)$$

³We are very grateful to Domagoj Leljak providing us with the variances and correlation matrix of z -expansion parameters of $B_c \rightarrow J/\psi$ tensor form factors.

According to the following steps, we select a total of eight NP benchmark points under seven different NP hypotheses.

Switching one coupling C_i at a time, there are five NP hypotheses. The hypothesis of a single C_{V_L} can resolve the $R(D^{(*)})$ anomalies well, but there is no effect on the normalized observables defined in section 3, so we should not choose it. The hypothesis of a single C_{S_L} or C_{S_R} is ruled out by the decay rate of $B_c \rightarrow \tau\nu$ decay [28, 43, 98]. We take a benchmark point from each of the two remaining NP hypotheses as follows [22]

$$\begin{aligned} \text{BP1:} \quad & (\text{Re}[C_{V_R}], \text{Im}[C_{V_R}]) = (-0.030, 0.460) \\ \text{BP2:} \quad & (\text{Re}[C_T], \text{Im}[C_T]) = (0.011, 0.164) \end{aligned}$$

The corresponding complex conjugate fitting values $(\text{Re}[C_{V_R}], \text{Im}[C_{V_R}]) = (-0.030, -0.460)$ and $(\text{Re}[C_T], \text{Im}[C_T]) = (0.011, -0.164)$ are marked as BP1* and BP2*, respectively. Although BP1 (BP2) and BP1* (BP2*) are formally different benchmark points, they produce the same results for angular observables $\widehat{\mathcal{I}}_{1c,1s,2c,2s,6c,6s,3,4,5}$ and opposite results for $\widehat{\mathcal{I}}_{7,8,9}$. Observables $\widehat{\mathcal{I}}_{7,8,9}$ can distinguish between the NP benchmark point and its complex conjugate partner very well. In the following analysis, we do not consider BP1* and BP2*, and the same treatment is also applicable to the following BP6*, which is the complex conjugate of the benchmark point BP6.

Considering the combinations induced by specific UV models, we choose the best-fit points in the following four different NP hypotheses as our NP benchmark points (the remaining C_i are set to zero in each case) [21]

$$\begin{aligned} \text{BP3:} \quad & (C_{V_L}, C_{S_L} = -4C_T) = (0.10, -0.04) \\ \text{BP4:} \quad & (C_{S_R}, C_{S_L}) = (0.21, -0.15) \text{ (A)} \quad \text{or} \quad (-0.26, -0.61) \text{ (B)} \\ \text{BP5:} \quad & (C_{V_L}, C_{S_R}) = (0.08, -0.01) \\ \text{BP6:} \quad & (\text{Re}[C_{S_L} = 4C_T], \text{Im}[C_{S_L} = 4C_T]) = (-0.06, 0.31) \end{aligned}$$

where the Wilson coefficients are given at the NP scale 1TeV, and we should run them down to the scale m_b [20].

Finally, taking into account all NP Wilson coefficients, except C_{V_R} which is explicitly lepton-flavor universal in the standard model effective field theory formalism up to contributions of $\mathcal{O}(\mu_{\text{EW}}^4/\Lambda^4)$ [17], we choose a set of values labelled ‘‘Min 1b’’ in table 8 of ref. [19] as our NP benchmark point BP7

$$\text{BP7:} \quad (C_{V_L}, C_{S_R}, C_{S_L}, C_T) = (0.09, 0.086, -0.14, 0.008)$$

We adopt the same treatment as in many literatures (e.g. [49, 72, 99–101]), that is, only the central value of best-fit result is considered as the benchmark point to qualitatively discuss the influence of the NP effect.

4.3 Angular observables $\widehat{\mathcal{I}}_i(q^2)$

In figure 2, we show the predictions for entire set of angular observables $\widehat{\mathcal{I}}_i(q^2)$ within the SM and eight NP benchmark points. It is easy to see that the BP2 (corresponding to the

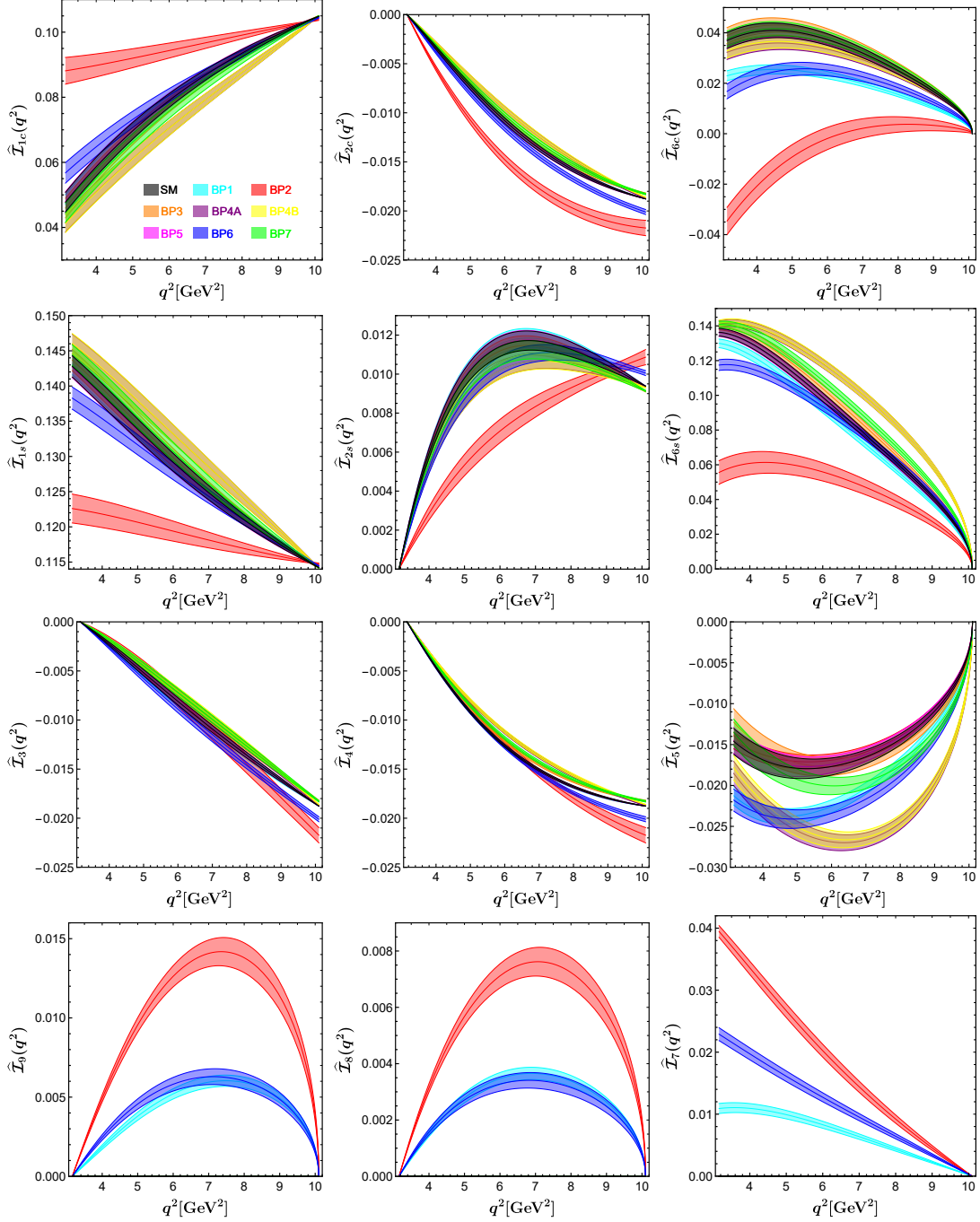


Figure 2. The angular observables $\widehat{\mathcal{L}}_i(q^2)$ as a function of q^2 , predicted both within the SM and in eight NP benchmark points. The width of each curve is derived from the theoretical uncertainties of $B_c \rightarrow J/\psi$ form factors.

red band in figure 2) has the greatest effect on all $\widehat{\mathcal{L}}_i(q^2)$ except $\widehat{\mathcal{L}}_5(q^2)$. The value of $\widehat{\mathcal{L}}_5(q^2)$ in BP2 is almost the same as that in the SM. The NP corresponding to BP2 even makes the angular observables $\widehat{\mathcal{L}}_{6c}(q^2)$ negative, which is not present in the SM and in other NP

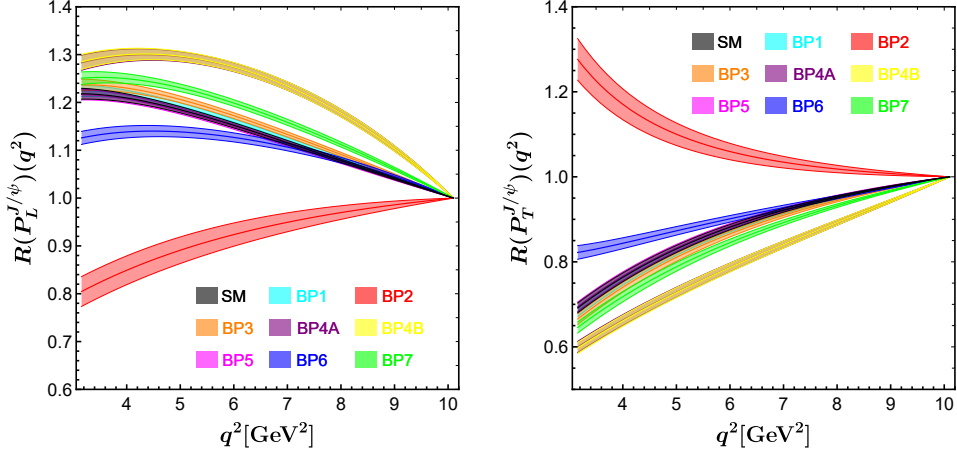


Figure 3. Lepton-flavor-universality ratios $R(P_{L,T}^{J/\psi})(q^2)$ as a function of q^2 , predicted both within the SM and in eight NP benchmark points. The width of each curve is derived from the theoretical uncertainties of $B_c \rightarrow J/\psi$ form factors.

benchmark points.

In the BP6 (corresponding to the blue band in figure 2), the contributions of NP to all $\widehat{\mathcal{L}}_i(q^2)$ except $\widehat{\mathcal{L}}_5(q^2)$ are in the same direction as in BP2, but the impacts are smaller than that in BP2. The BP6 can obviously decrease the value of $\widehat{\mathcal{L}}_5(q^2)$. Observables sensitive to BP6 can be used to study specific UV models, such as the scalar $SU(2)_L$ doublet S_2 (also called R_2) leptoquark [30], which can produce the relationship $C_{S_L} = 4C_T$ at the NP scale.

As we expected, only BP1, BP2, and BP6 which can provide complex phases can produce nonzero angular observables $\widehat{\mathcal{L}}_{7,8,9}(q^2)$. The BP1 (corresponding to the cyan band in figure 2) makes $\widehat{\mathcal{L}}_{5,6c,6s}(q^2)$ decrease slightly, and hardly contributes to $\widehat{\mathcal{L}}_{1c,1s,2c,2s,3,4}(q^2)$. The results of all $\widehat{\mathcal{L}}_i(q^2)$ predicted by BP4A and BP4B (corresponding to the purple and yellow bands in figure 2, respectively) almost completely coincide with each other. This indicates that $\widehat{\mathcal{L}}_i(q^2)$ cannot be used to distinguish the two best-fit points of NP hypothesis (C_{S_R}, C_{S_L}) , which is motivated by models with extra charged Higgs. This is different from the situation in the angular observables of $\Lambda_b^0 \rightarrow \Lambda_c^+(\rightarrow \Lambda^0 \pi^+) \tau^-(\rightarrow \pi^- \nu_\tau) \bar{\nu}_\tau$ decay, which can distinguish between BP4A and BP4B very well [74]. The BP4A and BP4B make $\widehat{\mathcal{L}}_{1c,2s,5,6c}(q^2)$ decrease slightly and $\widehat{\mathcal{L}}_{1s,2c,3,4,6s}(q^2)$ increase slightly. The NP effects of BP3, BP5, and BP7 have little impact on the $\widehat{\mathcal{L}}_i(q^2)$.

4.4 Lepton-flavor-universality ratios $R(P_{L,T}^{J/\psi})(q^2)$ and $R(J/\psi)$

The q^2 distribution of lepton-flavor-universality ratios $R(P_{L,T}^{J/\psi})$ are shown in figure 3, which includes the results within the SM and eight NP benchmark points. All NP benchmark points except BP5 and BP1 can be distinguished by $R(P_{L,T}^{J/\psi})(q^2)$, especially in the small q^2 region. The results of $R(P_{L,T}^{J/\psi})(q^2)$ predicted by BP4A and BP4B almost completely coincide with each other. The longitudinal polarization ratio $R(P_L^{J/\psi})(q^2)$ is decreased by benchmarks BP2 and BP6, and increased by benchmarks BP4A, BP4B, BP7, and BP3. Especially, the NP effect of BP2 makes the ratio $R(P_L^{J/\psi})(q^2)$ significantly less than 1. The

transverse polarization ratio $R(P_T^{J/\psi})(q^2)$ is increased by benchmarks BP2 and BP6, and decreased by benchmarks BP4A, BP4B, BP7, and BP3. The NP effect of BP2 makes the ratio $R(P_T^{J/\psi})(q^2)$ significantly greater than 1.

All of the NP benchmark points can increase the ratio $R(J/\psi)$. $R(J/\psi)$ does not use the τ channel for normalization, so the C_{V_L} contribution of BP3, BP5, and BP7 can be seen. The predicted values of $R(J/\psi)$ are shown as follows

$$\begin{aligned} R(J/\psi)_{\text{SM}} &= 0.2582(38), & R(J/\psi)_{\text{BP1}} &= 0.3272(50), & R(J/\psi)_{\text{BP2}} &= 0.3373(176), \\ R(J/\psi)_{\text{BP3}} &= 0.3030(45), & R(J/\psi)_{\text{BP4A}} &= 0.2781(36), & R(J/\psi)_{\text{BP4B}} &= 0.2754(36), \\ R(J/\psi)_{\text{BP5}} &= 0.3007(44), & R(J/\psi)_{\text{BP6}} &= 0.2938(67), & R(J/\psi)_{\text{BP7}} &= 0.3031(44). \end{aligned} \quad (4.2)$$

5 Symmetries in the angular observables without tensor operators

In the absence of tensor operators, the twelve angular observables $\mathcal{I}_i(q^2, E_\pi)$ defined in section 2.3 are not independent. These angular observables change to

$$\mathcal{I}_{1c} = S_1 \left(|\mathcal{A}_\perp|^2 + |\mathcal{A}_\parallel|^2 \right), \quad (5.1)$$

$$\mathcal{I}_{1s} = S_t |\mathcal{A}_t|^2 + (S_1 - S_3) |\mathcal{A}_0|^2 + \frac{1}{2} S_1 \left(|\mathcal{A}_\perp|^2 + |\mathcal{A}_\parallel|^2 \right), \quad (5.2)$$

$$\mathcal{I}_{2c} = S_3 \left(|\mathcal{A}_\perp|^2 + |\mathcal{A}_\parallel|^2 \right), \quad (5.3)$$

$$\mathcal{I}_{2s} = -2S_3 |\mathcal{A}_0|^2 + \frac{1}{2} S_3 \left(|\mathcal{A}_\perp|^2 + |\mathcal{A}_\parallel|^2 \right), \quad (5.4)$$

$$\mathcal{I}_{6c} = 2S_2 \text{Re} [\mathcal{A}_\parallel \mathcal{A}_\perp^*], \quad (5.5)$$

$$\mathcal{I}_{6s} = \text{Re} \left[S_2 \mathcal{A}_\parallel \mathcal{A}_\perp^* - \sqrt{2} R_t \mathcal{A}_t \mathcal{A}_0^* \right], \quad (5.6)$$

$$\mathcal{I}_3 = S_3 \left(|\mathcal{A}_\perp|^2 - |\mathcal{A}_\parallel|^2 \right), \quad (5.7)$$

$$\mathcal{I}_9 = 2S_3 \text{Im} [\mathcal{A}_\parallel \mathcal{A}_\perp^*], \quad (5.8)$$

$$\mathcal{I}_4 = \sqrt{2} S_3 \text{Re} [\mathcal{A}_\perp \mathcal{A}_0^*], \quad (5.9)$$

$$\mathcal{I}_8 = \sqrt{2} S_3 \text{Im} [\mathcal{A}_\parallel \mathcal{A}_0^*], \quad (5.10)$$

$$\mathcal{I}_5 = \frac{1}{2\sqrt{2}} \text{Re} \left[2S_2 \mathcal{A}_\parallel \mathcal{A}_0^* + \sqrt{2} R_t \mathcal{A}_t \mathcal{A}_\perp^* \right], \quad (5.11)$$

$$\mathcal{I}_7 = \frac{1}{2\sqrt{2}} \text{Im} \left[2S_2 \mathcal{A}_\perp \mathcal{A}_0^* - \sqrt{2} R_t \mathcal{A}_t \mathcal{A}_\parallel^* \right]. \quad (5.12)$$

We can consider these angular observables as being bilinear in

$$\vec{A} \equiv \{ \text{Re}[\mathcal{A}_t], \text{Im}[\mathcal{A}_t], \text{Re}[\mathcal{A}_0], \text{Im}[\mathcal{A}_0], \text{Re}[\mathcal{A}_\perp], \text{Im}[\mathcal{A}_\perp], \text{Re}[\mathcal{A}_\parallel], \text{Im}[\mathcal{A}_\parallel] \}. \quad (5.13)$$

Generally, the experimental and theoretical degrees of freedom can be matched by the following formula [101–104]

$$n_c - n_d = 2n_A - n_s, \quad (5.14)$$

where n_c is the number of angular observables \mathcal{I}_i . n_d is the number of dependencies between the different observables \mathcal{I}_i , which can be obtained by the difference between the number

of observables \mathcal{I}_i and the dimension of the space given by the gradient vectors $\vec{\nabla}\mathcal{I}_i$ (with the derivatives taken with respect to the various elements of \vec{A}). n_A is the number of transversity amplitudes (each \mathcal{A}_j is complex and therefore has two degrees of freedom). n_s is the number of continuous symmetries.

Without tensor operators, there are still twelve angular observables \mathcal{I}_i but only four amplitudes $\mathcal{A}_{t,0,\perp,\parallel}$. So $n_c = 12$ and $n_A = 4$. In this case, the only continuous symmetry that can be found is

$$\mathcal{A}_t \rightarrow e^{i\alpha} \mathcal{A}_t, \quad \mathcal{A}_0 \rightarrow e^{i\alpha} \mathcal{A}_0, \quad \mathcal{A}_\perp \rightarrow e^{i\alpha} \mathcal{A}_\perp, \quad \mathcal{A}_\parallel \rightarrow e^{i\alpha} \mathcal{A}_\parallel. \quad (5.15)$$

Only 7 of the 12 angular observables \mathcal{I}_i are independent and 5 dependencies are found. We present the dependence relations directly here and provide the detailed derivation in appendix B.

$$S_1 \mathcal{I}_{2c} = S_3 \mathcal{I}_{1c}, \quad (5.16)$$

$$S_2^2 \mathcal{I}_{2c}^2 = S_2^2 (\mathcal{I}_3^2 + \mathcal{I}_9^2) + S_3^2 \mathcal{I}_{6c}^2, \quad (5.17)$$

$$4S_2^2 \beta_2^2 = S_3^2 \mathcal{I}_{6c}^2 [(\mathcal{I}_{2c} - 2\mathcal{I}_{2s})(\mathcal{I}_{2c} + \mathcal{I}_3) - 4\mathcal{I}_4^2], \quad (5.18)$$

$$\begin{aligned} R_t^2 (\mathcal{I}_{2c} - 2\mathcal{I}_{2s}) [4S_3 \mathcal{I}_{1s} + (S_3 - 3S_1) \mathcal{I}_{2c} + 2(S_1 - S_3) \mathcal{I}_{2s}] \\ = 2S_t \left\{ S_3^2 (\mathcal{I}_{6c} - 2\mathcal{I}_{6s})^2 + \frac{[S_3^2 \mathcal{I}_{6c} \beta_3 + S_2^2 (\mathcal{I}_{2c} - 2\mathcal{I}_{2s}) \mathcal{I}_9 \beta_2]^2}{S_2^2 (\mathcal{I}_{2c} + \mathcal{I}_3)^2 \beta_2^2} \right\}, \end{aligned} \quad (5.19)$$

$$\begin{aligned} 2S_3^2 (\mathcal{I}_{2c} + \mathcal{I}_3)^2 \mathcal{I}_7 = S_2^2 \frac{[(\mathcal{I}_{2c} + \mathcal{I}_3)^2 + \mathcal{I}_9^2] \beta_2}{\mathcal{I}_{6c}} - \frac{S_3^4 \mathcal{I}_4 \mathcal{I}_{6c}^2 \beta_3}{S_2^2 (\mathcal{I}_{2c} - 2\mathcal{I}_{2s}) \beta_2} \\ + S_3^2 \frac{\mathcal{I}_9 [\beta_3 - (\mathcal{I}_{2c} - 2\mathcal{I}_{2s}) \mathcal{I}_4 \mathcal{I}_{6c}] + \mathcal{I}_8 (\mathcal{I}_{2c} + \mathcal{I}_3)^2 (\mathcal{I}_{6c} - 2\mathcal{I}_{6s})}{\mathcal{I}_{2c} - 2\mathcal{I}_{2s}}, \end{aligned} \quad (5.20)$$

with

$$\beta_2 \equiv (\mathcal{I}_{2c} + \mathcal{I}_3) \mathcal{I}_8 - \mathcal{I}_4 \mathcal{I}_9, \quad (5.21)$$

$$\begin{aligned} \beta_3 \equiv 2\mathcal{I}_{2c} \mathcal{I}_5 (\mathcal{I}_{2c} - 2\mathcal{I}_{2s} + \mathcal{I}_3) + 2\mathcal{I}_4 \mathcal{I}_{6s} (\mathcal{I}_{2c} + \mathcal{I}_3) \\ + \mathcal{I}_4 \mathcal{I}_{6c} (2\mathcal{I}_{2s} - \mathcal{I}_3 - 2\mathcal{I}_{2c}) - 4\mathcal{I}_{2s} \mathcal{I}_3 \mathcal{I}_5. \end{aligned} \quad (5.22)$$

Eqs. (5.16)–(5.20) can be used as a model-independent method to determine the existence of tensor operators. The “model-independent method” here not only means that it does not depend on the NP models, but also means that it does not depend on the calculation of $B_c \rightarrow J/\psi$ transition form factors.

Furthermore, we can obtain the dependence relations among the normalized angular observables $\widehat{\mathcal{I}}_i(q^2)$ by replacing the $\mathcal{I}_i(q^2, E_\pi)$ and the dimensionless factors $S_{t,1,2,3}$ and R_t in eqs. (5.16)–(5.22) with $\widehat{\mathcal{I}}_i(q^2)$, $\bar{S}_{t,1,2,3}$ and \bar{R}_t , respectively. The factors $\bar{S}_{t,1,2,3}$ and \bar{R}_t are respectively defined as

$$\bar{S}_{t,1,2,3} \equiv \int S_{t,1,2,3} dE_\pi, \quad \bar{R}_t \equiv \int R_t dE_\pi. \quad (5.23)$$

6 Conclusions

Inspired by the $R(D^{(*)})$ anomalies, the angular distribution of $B_c^- \rightarrow J/\psi \tau^- \bar{\nu}_\tau$ or $B_c^- \rightarrow J/\psi (\rightarrow \mu^+ \mu^-) \tau^- \bar{\nu}_\tau$ decay has been used to explore possible NP patterns in $b \rightarrow c \tau^- \bar{\nu}_\tau$ transition in many previous works. However, angular observables depending on the solid angle of final-state τ^- are unmeasurable theoretically, since the decay products of τ^- inevitably contain an undetected ν_τ and the solid angle of τ^- cannot be determined precisely. Therefore, in this work, we study the *measurable* angular distribution of the five-body decay $B_c^- \rightarrow J/\psi (\rightarrow \mu^+ \mu^-) \tau^- (\rightarrow \pi^- \nu_\tau) \bar{\nu}_\tau$, which includes three visible final-state particles μ^+ , μ^- , and π^- whose three-momenta can be measured.

The five-fold differential decay rate containing all NP effective operators can be expressed in terms of twelve angular observables $\mathcal{I}_i(q^2, E_\pi)$, which can be completely expressed by seven independent transversity amplitudes and some dimensionless factors. As long as one of the angular observables \mathcal{I}_7 , \mathcal{I}_8 and \mathcal{I}_9 is nonzero, this will be an unquestionable sign of NP, and indicates that the NP can cause extra weak phases. Integrating over the E_π and after normalization of $d\Gamma/dq^2$, we construct twelve normalized angular observables $\widehat{\mathcal{I}}_i(q^2)$. By integrating over all lepton-side parameters, We find there are only two angular observables $P_{L,T}^{J/\psi}(q^2)$ whose determination can be obtained without reconstruction of the dilepton solid angle. The $P_{L,T}^{J/\psi}(q^2)$ are not affected by lepton dynamics, so they can be used to construct the ratios $R(P_{L,T}^{J/\psi})$ to probe the universality of lepton flavor.

Using the $B_c \rightarrow J/\psi$ vector and axial-vector form factors calculated by the latest lattice QCD and the tensor form factors calculated by the QCD sum rule, we predict the q^2 distribution of the twelve normalized angular observables $\widehat{\mathcal{I}}_i$ and the two lepton-flavor-universality ratios $R(P_{L,T}^{J/\psi})$ both within the SM and in eight NP benchmark points, which are a variety of best-fit points in seven different NP hypotheses. We find that the benchmark BP2 (corresponding to the hypothesis of tensor operator) has the greatest effect on all $\widehat{\mathcal{I}}_i$ and $R(P_{L,T}^{J/\psi})$, except $\widehat{\mathcal{I}}_5$. Especially for the observables $\widehat{\mathcal{I}}_{6c}$ and $R(P_{L,T}^{J/\psi})$, BP2 makes their predictions very different from those in the SM and other benchmark points. The results of all $\widehat{\mathcal{I}}_i$ and $R(P_{L,T}^{J/\psi})$ predicted by the two best-fit points (i.e. BP4A and BP4B) of NP hypothesis (C_{S_R}, C_{S_L}) , which is motivated by models with extra charged Higgs, almost completely coincide with each other. This is different from the situation in the angular observables of the baryonic counterparts, which can distinguish between BP4A and BP4B very well. In addition to the benchmarks BP2, BP4A, and BP4B, the BP1, BP6, and BP7 can also have some influence on the observables. Compared with the $\widehat{\mathcal{I}}_i$, the ratios $R(P_{L,T}^{J/\psi})$ are more sensitive to the NP with pseudo-scalar operator. All NP benchmark points can improve the value of $R(J/\psi)$, which makes it closer to the experimental measurement.

Finally, we discuss the symmetries in the angular observables without tensor operators, and present five dependence relations. Once all twelve angular observables are measured, these five relations will be a very useful way to determine the existence of tensor operators. If these relations are not fulfilled, it means that there must be tensor operators. This method is completely independent of any assumptions on the details of the NP model and $B_c \rightarrow J/\psi$ transition form factors. Future precise measurements of the angular observables in $B_c^- \rightarrow J/\psi (\rightarrow \mu^+ \mu^-) \tau^- (\rightarrow \pi^- \nu_\tau) \bar{\nu}_\tau$ decay, especially precise measurements of the

normalized ones, would be very helpful to provide a more definite answer concerning the anomalies observed in $b \rightarrow c\tau^-\bar{\nu}_\tau$ transition, restricting further or even deciphering the NP models.

Acknowledgments

This work is supported by the National Natural Science Foundation of China under Grant Nos. 11947083, 12075097, 11675061 and 11775092, as well as by the CCNU-QLPL Innovation Fund (QLPL2020P01). X.L. is also supported by the Fundamental Research Funds for the Central Universities under Grant No. CCNU20TS007.

A The calculation of the angular distribution

In the appendix of ref. [74], we have given the detailed calculation procedures for the similar five-body cascade decay of unpolarized Λ_b baryon. The calculation of $V^* \rightarrow \tau^-(\rightarrow \pi^-\nu_\tau)\bar{\nu}_\tau$ part is exactly the same as that in this work. Therefore, in this section, we mainly present some important definitions and conventions, and calculate the $J/\psi \rightarrow \mu^+\mu^-$ decay. At the end of this section, the dimensionless factors are listed for the sake of completeness of this paper.

A.1 Definitions and conventions

The differential decay rate of cascade decay $B_c^- \rightarrow J/\psi(\rightarrow \mu^+\mu^-)\tau^-(\rightarrow \pi^-\nu_\tau)\bar{\nu}_\tau$ can be written as

$$d\Gamma = \frac{4G_F^2 |V_{cb}|^2 \mathcal{B}(\tau \rightarrow \pi^-\nu_\tau) dq^2}{m_{B_c} (m_\tau^2 - m_\pi^2)^2 m_{J/\psi} \Gamma_{J/\psi}} \sum_{\lambda_{\mu^-}, \lambda_{\mu^+}} \left| \mathcal{M}_{\lambda_{\mu^-}, \lambda_{\mu^+}} \right|^2 d\Pi_2(p_{B_c}; q, p_{J/\psi}) \times d\Pi_2(q; p_\tau, p_{\bar{\nu}}) d\Pi_2(p_\tau; p_{\pi^-}, p_\nu) d\Pi_2(p_{J/\psi}; p_{\mu^-}, p_{\mu^+}), \quad (\text{A.1})$$

where

$$\mathcal{M}_{\lambda_{\mu^-}, \lambda_{\mu^+}} \equiv \mathcal{H}_{\lambda_{\mu^-}, \lambda_{\mu^+}} \mathcal{L} + \sum_{\lambda} \eta_{\lambda} \mathcal{H}_{\lambda_{\mu^-}, \lambda_{\mu^+}}^{\lambda} \mathcal{L}_{\lambda} + \sum_{\lambda, \lambda'} \eta_{\lambda} \eta_{\lambda'} \mathcal{H}_{\lambda_{\mu^-}, \lambda_{\mu^+}}^{\lambda, \lambda'} \mathcal{L}_{\lambda, \lambda'}, \quad (\text{A.2})$$

$$\mathcal{H}_{\lambda_{\mu^-}, \lambda_{\mu^+}} = \sum_{\lambda_{J/\psi}} H_{\lambda_{J/\psi}} \mathcal{M}_{\lambda_{\mu^-}, \lambda_{\mu^+}}^{\lambda_{J/\psi}}, \quad (\text{A.3})$$

$$\mathcal{H}_{\lambda_{\mu^-}, \lambda_{\mu^+}}^{\lambda} = \sum_{\lambda_{J/\psi}} H_{\lambda_{J/\psi}}^{\lambda} \mathcal{M}_{\lambda_{\mu^-}, \lambda_{\mu^+}}^{\lambda_{J/\psi}}, \quad (\text{A.4})$$

$$\mathcal{H}_{\lambda_{\mu^-}, \lambda_{\mu^+}}^{\lambda, \lambda'} = \sum_{\lambda_{J/\psi}} H_{\lambda_{J/\psi}}^{\lambda, \lambda'} \mathcal{M}_{\lambda_{\mu^-}, \lambda_{\mu^+}}^{\lambda_{J/\psi}}. \quad (\text{A.5})$$

The λ_{μ^-} and λ_{μ^+} respectively represent the helicity of final-state particles μ^- and μ^+ , as well as the $\lambda^{(\prime)}$ and $\lambda_{J/\psi}$ respectively represent the helicity of intermediate state V^* and J/ψ . The $d\Pi_2$ stands for the two-body phase space. $\mathcal{M}_{\lambda_{\mu^-}, \lambda_{\mu^+}}^{\lambda_{J/\psi}}$ denotes the helicity

amplitude related to $J/\psi \rightarrow \mu^+\mu^-$ decay. $H_{\lambda_{J/\psi}}^{(\lambda,\lambda')}$ are the hadronic helicity amplitudes describing the $B_c \rightarrow J/\psi$ transition with different Lorentz structures.

$$H_{\lambda_{J/\psi}} = \langle J/\psi(\lambda_{J/\psi}) | g_S(\bar{c}b) + g_P(\bar{c}\gamma_5 b) | B_c \rangle, \quad (\text{A.6})$$

$$H_{\lambda_{J/\psi}}^\lambda = \epsilon^{\mu*}(\lambda) \langle J/\psi(\lambda_{J/\psi}) | g_V(\bar{c}\gamma_\mu b) + g_A(\bar{c}\gamma_\mu\gamma_5 b) | B_c \rangle, \quad (\text{A.7})$$

$$H_{\lambda_{J/\psi}}^{\lambda,\lambda'} = g_T \epsilon^{\mu*}(\lambda) \epsilon^{\nu*}(\lambda') \langle J/\psi(\lambda_{J/\psi}) | \bar{c}i\sigma_{\mu\nu}(1 - \gamma_5)b | B_c \rangle, \quad (\text{A.8})$$

where $\epsilon^\mu(\lambda)$ denotes the polarization vector of the virtual vector boson V^* with helicity λ . The modified leptonic helicity amplitudes are $L_{(\lambda,\lambda')}$, which can be obtained directly from the appendix of ref. [74].

In the B_c rest frame, the polarization vector of J/ψ meson can be written as [105, 106]

$$\varepsilon^\mu(\pm 1) = (0, \mp 1, -i, 0) / \sqrt{2}, \quad (\text{A.9})$$

$$\varepsilon^\mu(0) = (|\mathbf{p}_{J/\psi}|, 0, 0, E_{J/\psi}) / m_{J/\psi}, \quad (\text{A.10})$$

with $|\mathbf{p}_{J/\psi}| = \sqrt{Q_+Q_-} / (2m_{B_c})$ and $E_{J/\psi} = (m_{B_c}^2 + m_{J/\psi}^2 - q^2) / (2m_{B_c})$. The polarization vector of virtual V^* can be written as [105, 106]

$$\epsilon^\mu(\pm 1) = (0, \pm 1, -i, 0) / \sqrt{2}, \quad (\text{A.11})$$

$$\epsilon^\mu(0) = (|\mathbf{q}|, 0, 0, -q_0) / \sqrt{q^2}, \quad (\text{A.12})$$

$$\epsilon^\mu(t) = q^\mu / \sqrt{q^2}, \quad (\text{A.13})$$

with $|\mathbf{q}| = \sqrt{Q_+Q_-} / (2m_{B_c})$ and $q_0 = (m_{B_c}^2 - m_{J/\psi}^2 + q^2) / (2m_{B_c})$. The eqs. (A.11)–(A.13) satisfy the completeness relation

$$g^{\mu\nu} = \sum_{\lambda \in \{t, \pm 1, 0\}} \epsilon^\mu(\lambda) \epsilon^{\nu*}(\lambda) \eta_\lambda, \quad (\text{A.14})$$

where $\eta_t = 1$ and $\eta_{\pm 1, 0} = -1$.

For scalar and pseudo-scalar operators, there is only one nonzero hadronic helicity amplitude

$$H_0 = \mathcal{A}_t^{SP}. \quad (\text{A.15})$$

For vector and axial-vector operators, there are four nonzero hadronic helicity amplitudes listed as follows

$$\begin{aligned} H_0^t &= \mathcal{A}_t^{VA}, & H_0^0 &= \mathcal{A}_0, \\ H_1^1 &= (\mathcal{A}_\perp + \mathcal{A}_\parallel) / \sqrt{2}, & H_{-1}^{-1} &= (\mathcal{A}_\perp - \mathcal{A}_\parallel) / \sqrt{2}. \end{aligned} \quad (\text{A.16})$$

For the tensor operators, there are twelve nonzero hadronic helicity amplitudes listed as follows

$$\begin{aligned} H_0^{t,0} &= H_0^{-1,1} = -H_0^{0,t} = -H_0^{1,-1} = \mathcal{A}_0^T, \\ H_1^{0,1} &= H_1^{t,1} = -H_1^{1,0} = -H_1^{1,t} = (\mathcal{A}_\parallel^T + \mathcal{A}_\perp^T) / \sqrt{2}, \\ H_{-1}^{0,-1} &= H_{-1}^{-1,t} = -H_{-1}^{-1,0} = -H_{-1}^{t,-1} = (\mathcal{A}_\parallel^T - \mathcal{A}_\perp^T) / \sqrt{2}. \end{aligned} \quad (\text{A.17})$$

A.2 Calculating $J/\psi \rightarrow \mu^+ \mu^-$ decay

The $J/\psi \rightarrow \mu^+ \mu^-$ decay should be calculated in the J/ψ rest frame. In this reference frame, the transverse polarization vector of J/ψ meson does not change, i.e., $\tilde{\varepsilon}^\mu(\pm 1) = \varepsilon^\mu(\pm 1)$, but its longitudinal polarization vector changes to $\tilde{\varepsilon}^\mu(0) = (0, 0, 0, 1)$. For massless μ^- and μ^+ leptons, their spinors can be written as [105, 106]

$$u\left(\frac{1}{2}\right) = \sqrt{\frac{m_{J/\psi}}{2}} \left(\cos \frac{\theta_{J/\psi}}{2}, \sin \frac{\theta_{J/\psi}}{2}, \cos \frac{\theta_{J/\psi}}{2}, \sin \frac{\theta_{J/\psi}}{2} \right)^T, \quad (\text{A.18})$$

$$u\left(-\frac{1}{2}\right) = \sqrt{\frac{m_{J/\psi}}{2}} \left(-\sin \frac{\theta_{J/\psi}}{2}, \cos \frac{\theta_{J/\psi}}{2}, \sin \frac{\theta_{J/\psi}}{2}, -\cos \frac{\theta_{J/\psi}}{2} \right)^T, \quad (\text{A.19})$$

$$v\left(\frac{1}{2}\right) = \sqrt{\frac{m_{J/\psi}}{2}} \left(\cos \frac{\theta_{J/\psi}}{2}, \sin \frac{\theta_{J/\psi}}{2}, -\cos \frac{\theta_{J/\psi}}{2}, -\sin \frac{\theta_{J/\psi}}{2} \right)^T, \quad (\text{A.20})$$

$$v\left(-\frac{1}{2}\right) = \sqrt{\frac{m_{J/\psi}}{2}} \left(-\sin \frac{\theta_{J/\psi}}{2}, \cos \frac{\theta_{J/\psi}}{2}, -\sin \frac{\theta_{J/\psi}}{2}, \cos \frac{\theta_{J/\psi}}{2} \right)^T, \quad (\text{A.21})$$

where the Jacob-Wick second particle convention has been used [107].

Due to the $J/\psi \rightarrow \mu^+ \mu^-$ decay is dominated by electromagnetic interaction, we can write the helicity amplitude as follows

$$\mathcal{M}_{\lambda_{\mu^-}, \lambda_{\mu^+}}^{\lambda_{J/\psi}}(J/\psi \rightarrow \mu^+ \mu^-) = N_{J/\psi} \tilde{\varepsilon}_{J/\psi}^\mu(\lambda_{J/\psi}) \bar{u}(\lambda_{\mu^-}) \gamma_\mu v(\lambda_{\mu^+}), \quad (\text{A.22})$$

where $N_{J/\psi} \equiv -8i\pi\alpha_{\text{EM}}f_{J/\psi}/(3m_{J/\psi})$, $f_{J/\psi}$ is the decay constant of J/ψ meson, α_{EM} is the fine-structure constant. There are six nonzero helicity amplitudes as follows

$$\mathcal{M}_{\frac{1}{2}, -\frac{1}{2}}^1 = \mathcal{M}_{-\frac{1}{2}, \frac{1}{2}}^{-1} = \frac{N_{J/\psi} m_{J/\psi}}{\sqrt{2}} (1 + \cos \theta_{J/\psi}), \quad (\text{A.23})$$

$$\mathcal{M}_{\frac{1}{2}, -\frac{1}{2}}^{-1} = \mathcal{M}_{-\frac{1}{2}, \frac{1}{2}}^1 = \frac{N_{J/\psi} m_{J/\psi}}{\sqrt{2}} (1 - \cos \theta_{J/\psi}), \quad (\text{A.24})$$

$$\mathcal{M}_{\frac{1}{2}, -\frac{1}{2}}^0 = -\mathcal{M}_{-\frac{1}{2}, \frac{1}{2}}^0 = N_{J/\psi} m_{J/\psi} \sin \theta_{J/\psi}, \quad (\text{A.25})$$

and one can obtain that the total decay rate is

$$\Gamma(J/\psi \rightarrow \mu^+ \mu^-) = \frac{|N_{J/\psi}|^2 m_{J/\psi}}{12\pi}. \quad (\text{A.26})$$

A.3 Dimensionless factors

The dimensionless factors induced in the calculation of $V^* \rightarrow \tau^-(\rightarrow \pi^- \nu_\tau) \bar{\nu}_\tau$ are as follows [74]

$$S_t = 2\omega_\pi \kappa_\tau^2 - \kappa_\tau^4 - \kappa_\pi^2, \quad (\text{A.27})$$

$$S_1 = \frac{\kappa_\tau^2}{8(\omega_\pi^2 - \kappa_\pi^2)} \left[\kappa_\pi^2 (-6\omega_\pi \kappa_\tau^2 + 3\kappa_\tau^4 + 4\omega_\pi^2 + 10\omega_\pi - 5) \right. \\ \left. + (2\omega_\pi - \kappa_\tau^2) (2\omega_\pi^2 + 2\omega_\pi - 1) \kappa_\tau^2 - 3\kappa_\pi^4 + 6(1 - 2\omega_\pi) \omega_\pi^2 \right], \quad (\text{A.28})$$

$$S_2 = \frac{\kappa_\tau^2 (\kappa_\pi^2 - 2\omega_\pi + 1) (\omega_\pi - \kappa_\tau^2)}{\sqrt{\omega_\pi^2 - \kappa_\pi^2}}, \quad (\text{A.29})$$

$$S_3 = \frac{\kappa_\tau^2}{8(\omega_\pi^2 - \kappa_\pi^2)} \left[\kappa_\pi^2 (-2\omega_\pi \kappa_\tau^2 + \kappa_\tau^4 + 4\omega_\pi^2 - 2\omega_\pi + 1) \right. \\ \left. + (\kappa_\tau^2 - 2\omega_\pi) (2\omega_\pi^2 - 6\omega_\pi + 3) \kappa_\tau^2 - \kappa_\pi^4 + 2(1 - 2\omega_\pi) \omega_\pi^2 \right], \quad (\text{A.30})$$

$$S_1^T = \frac{1}{2(\kappa_\pi^2 - \omega_\pi^2)} \left\{ \kappa_\pi^4 (2\omega_\pi \kappa_\tau^2 + 5\kappa_\tau^4 + 2\omega_\pi - 3) + 4\omega_\pi^2 \kappa_\tau^2 [(3\omega_\pi - 1) \kappa_\tau^2 - \omega_\pi] \right. \\ \left. + \kappa_\pi^2 [(-6\omega_\pi^2 - 10\omega_\pi + 3) \kappa_\tau^4 + 2(3 - 2\omega_\pi) \omega_\pi \kappa_\tau^2 + 2\omega_\pi^2] - \kappa_\pi^6 \right\}, \quad (\text{A.31})$$

$$S_2^T = \frac{4\kappa_\tau^2 (\kappa_\pi^2 - 2\omega_\pi + 1) (\kappa_\pi^2 - \omega_\pi \kappa_\tau^2)}{\sqrt{\omega_\pi^2 - \kappa_\pi^2}}, \quad (\text{A.32})$$

$$S_3^T = \frac{1}{2(\omega_\pi^2 - \kappa_\pi^2)} \left\{ \kappa_\pi^4 (-6\omega_\pi \kappa_\tau^2 + \kappa_\tau^4 - 6\omega_\pi + 1) - 4\omega_\pi^2 \kappa_\tau^2 [(\omega_\pi - 1) \kappa_\tau^2 + \omega_\pi] \right. \\ \left. + \kappa_\pi^2 [(2\omega_\pi^2 - 2\omega_\pi - 1) \kappa_\tau^4 + 2\omega_\pi (6\omega_\pi - 1) \kappa_\tau^2 + 2\omega_\pi^2] + 3\kappa_\pi^6 \right\}, \quad (\text{A.33})$$

$$R_t = \frac{\sqrt{2}(\omega_\pi - 1) \kappa_\tau (2\omega_\pi \kappa_\tau^2 - \kappa_\tau^4 - \kappa_\pi^2)}{\sqrt{\omega_\pi^2 - \kappa_\pi^2}}, \quad (\text{A.34})$$

$$R_t^T = \frac{2\sqrt{2}(\kappa_\pi^2 - \omega_\pi) (-2\omega_\pi \kappa_\tau^2 + \kappa_\tau^4 + \kappa_\pi^2)}{\sqrt{\omega_\pi^2 - \kappa_\pi^2}}, \quad (\text{A.35})$$

$$R_1 = \frac{\kappa_\tau}{2(\kappa_\pi^2 - \omega_\pi^2)} \left\{ \kappa_\pi^2 [(\omega_\pi + 2) \kappa_\tau^4 + (4\omega_\pi^2 + 8\omega_\pi - 6) \kappa_\tau^2 - 4\omega_\pi^2 + \omega_\pi] \right. \\ \left. + \kappa_\pi^4 (-6\kappa_\tau^2 + \omega_\pi + 2) + \omega_\pi \kappa_\tau^2 [(1 - 4\omega_\pi) \kappa_\tau^2 - 4(\omega_\pi - 1) \omega_\pi] \right\}, \quad (\text{A.36})$$

$$R_2 = \frac{2\kappa_\tau (\kappa_\tau^4 - \kappa_\pi^2) (\kappa_\pi^2 - 2\omega_\pi + 1)}{\sqrt{\omega_\pi^2 - \kappa_\pi^2}}, \quad (\text{A.37})$$

$$R_3 = \frac{\kappa_\tau}{2(\kappa_\pi^2 - \omega_\pi^2)} \left\{ \kappa_\pi^2 [(3\omega_\pi - 2) \kappa_\tau^4 + (-4\omega_\pi^2 + 8\omega_\pi - 2) \kappa_\tau^2 + (3 - 4\omega_\pi) \omega_\pi] \right. \\ \left. + \kappa_\pi^4 (-2\kappa_\tau^2 + 3\omega_\pi - 2) + \omega_\pi \kappa_\tau^2 [(3 - 4\omega_\pi) \kappa_\tau^2 + 4(\omega_\pi - 1) \omega_\pi] \right\}, \quad (\text{A.38})$$

where the three dimensionless parameters are defined as

$$\kappa_\tau \equiv \frac{m_\tau}{\sqrt{q^2}}, \quad \kappa_\pi \equiv \frac{m_\pi}{\sqrt{q^2}}, \quad \omega_\pi \equiv \frac{E_\pi}{\sqrt{q^2}}. \quad (\text{A.39})$$

B The detailed derivation of the dependence relations

In this section we provide the detailed derivation of the dependence relations among the angular observables \mathcal{I}_i . It is useful to re-express $\text{Im}[\mathcal{A}_\parallel \mathcal{A}_0^*]$, $\text{Re}[\mathcal{A}_\parallel \mathcal{A}_0^*]$, $\text{Re}[\mathcal{A}_t \mathcal{A}_\perp^*]$ and $\text{Im}[\mathcal{A}_t \mathcal{A}_\parallel^*]$ as

$$\text{Im}[\mathcal{A}_\parallel \mathcal{A}_0^*] = \frac{1}{|\mathcal{A}_\perp|^2} \left\{ \text{Im}[\mathcal{A}_\parallel \mathcal{A}_\perp^*] \text{Re}[\mathcal{A}_0 \mathcal{A}_\perp^*] - \text{Re}[\mathcal{A}_\parallel \mathcal{A}_\perp^*] \text{Im}[\mathcal{A}_0 \mathcal{A}_\perp^*] \right\}, \quad (\text{B.1})$$

$$\text{Re}[\mathcal{A}_\parallel \mathcal{A}_0^*] = \frac{1}{|\mathcal{A}_\perp|^2} \left\{ \text{Re}[\mathcal{A}_\parallel \mathcal{A}_\perp^*] \text{Re}[\mathcal{A}_0 \mathcal{A}_\perp^*] + \text{Im}[\mathcal{A}_\parallel \mathcal{A}_\perp^*] \text{Im}[\mathcal{A}_0 \mathcal{A}_\perp^*] \right\}, \quad (\text{B.2})$$

$$\text{Re}[\mathcal{A}_t \mathcal{A}_\perp^*] = \frac{1}{|\mathcal{A}_0|^2} \left\{ \text{Re}[\mathcal{A}_t \mathcal{A}_0^*] \text{Re}[\mathcal{A}_0 \mathcal{A}_\perp^*] - \text{Im}[\mathcal{A}_t \mathcal{A}_0^*] \text{Im}[\mathcal{A}_0 \mathcal{A}_\perp^*] \right\}, \quad (\text{B.3})$$

$$\begin{aligned}
\text{Im} [\mathcal{A}_t \mathcal{A}_\parallel^*] &= \frac{1}{|\mathcal{A}_0|^2 |\mathcal{A}_\perp|^2} \left\{ -\text{Re} [\mathcal{A}_t \mathcal{A}_0^*] \text{Re} [\mathcal{A}_0 \mathcal{A}_\perp^*] \text{Im} [\mathcal{A}_\parallel \mathcal{A}_\perp^*] \right. \\
&\quad + \text{Re} [\mathcal{A}_t \mathcal{A}_0^*] \text{Im} [\mathcal{A}_0 \mathcal{A}_\perp^*] \text{Re} [\mathcal{A}_\parallel \mathcal{A}_\perp^*] + \text{Im} [\mathcal{A}_t \mathcal{A}_0^*] \text{Re} [\mathcal{A}_0 \mathcal{A}_\perp^*] \text{Re} [\mathcal{A}_\parallel \mathcal{A}_\perp^*] \\
&\quad \left. + \text{Im} [\mathcal{A}_t \mathcal{A}_0^*] \text{Im} [\mathcal{A}_0 \mathcal{A}_\perp^*] \text{Im} [\mathcal{A}_\parallel \mathcal{A}_\perp^*] \right\}. \tag{B.4}
\end{aligned}$$

Therefore, the twelve angular observables (5.1)–(5.12) can be seen as functions of 4 real variables $|\mathcal{A}_t|^2$, $|\mathcal{A}_\perp|^2$, $|\mathcal{A}_\parallel|^2$, $|\mathcal{A}_0|^2$ and 3 complex variables $\mathcal{A}_t \mathcal{A}_0^*$, $\mathcal{A}_0 \mathcal{A}_\perp^*$, $\mathcal{A}_\parallel \mathcal{A}_\perp^*$. The advantage of this view is that it implies the continuous symmetry (5.15). There are only seven independent real variables due to the following three relationships

$$\text{Re} [\mathcal{A}_t \mathcal{A}_0^*]^2 + \text{Im} [\mathcal{A}_t \mathcal{A}_0^*]^2 = |\mathcal{A}_t|^2 |\mathcal{A}_0|^2, \tag{B.5}$$

$$\text{Re} [\mathcal{A}_0 \mathcal{A}_\perp^*]^2 + \text{Im} [\mathcal{A}_0 \mathcal{A}_\perp^*]^2 = |\mathcal{A}_0|^2 |\mathcal{A}_\perp|^2, \tag{B.6}$$

$$\text{Re} [\mathcal{A}_\parallel \mathcal{A}_\perp^*]^2 + \text{Im} [\mathcal{A}_\parallel \mathcal{A}_\perp^*]^2 = |\mathcal{A}_\parallel|^2 |\mathcal{A}_\perp|^2. \tag{B.7}$$

Inverting the eqs. (5.2)–(5.11), one can rewrite the variables in terms of the angular observables \mathcal{I}_i as follows

$$|\mathcal{A}_t|^2 = \frac{1}{S_t} \left[\mathcal{I}_{1s} + \frac{S_1 - S_3}{2S_3} \mathcal{I}_{2s} - \frac{3S_1 - S_3}{4S_3} \mathcal{I}_{2c} \right], \tag{B.8}$$

$$|\mathcal{A}_0|^2 = \frac{1}{4S_3} (\mathcal{I}_{2c} - 2\mathcal{I}_{2s}), \tag{B.9}$$

$$|\mathcal{A}_\perp|^2 = \frac{1}{2S_3} (\mathcal{I}_{2c} + \mathcal{I}_3), \tag{B.10}$$

$$|\mathcal{A}_\parallel|^2 = \frac{1}{2S_3} (\mathcal{I}_{2c} - \mathcal{I}_3), \tag{B.11}$$

$$\text{Re} [\mathcal{A}_t \mathcal{A}_0^*] = \frac{1}{2\sqrt{2}R_t} (\mathcal{I}_{6c} - 2\mathcal{I}_{6s}), \tag{B.12}$$

$$\text{Im} [\mathcal{A}_t \mathcal{A}_0^*] = \frac{S_3^2 \mathcal{I}_{6c} \beta_3 + S_2^2 \mathcal{I}_9 (\mathcal{I}_{2c} - 2\mathcal{I}_{2s}) \beta_2}{2\sqrt{2}R_t S_2 S_3 (\mathcal{I}_{2c} + \mathcal{I}_3) \beta_2}, \tag{B.13}$$

$$\text{Re} [\mathcal{A}_0 \mathcal{A}_\perp^*] = \frac{1}{\sqrt{2}S_3} \mathcal{I}_4, \tag{B.14}$$

$$\text{Im} [\mathcal{A}_0 \mathcal{A}_\perp^*] = -\frac{S_2}{\sqrt{2}S_3^2 \mathcal{I}_{6c}} \beta_2, \tag{B.15}$$

$$\text{Re} [\mathcal{A}_\parallel \mathcal{A}_\perp^*] = \frac{1}{2S_2} \mathcal{I}_{6c}, \tag{B.16}$$

$$\text{Im} [\mathcal{A}_\parallel \mathcal{A}_\perp^*] = \frac{1}{2S_3} \mathcal{I}_9, \tag{B.17}$$

with β_2 and β_3 defined in eqs. (5.21) and (5.22), respectively. Substituting them into eqs. (5.1), (5.12), and (B.5)–(B.7), we can obtain the final form of the 5 dependence relations (5.16)–(5.20).

References

- [1] ATLAS collaboration, *Observation of a new particle in the search for the Standard Model Higgs boson with the ATLAS detector at the LHC*, *Phys. Lett. B* **716** (2012) 1 [1207.7214].

- [2] CMS collaboration, *Observation of a New Boson at a Mass of 125 GeV with the CMS Experiment at the LHC*, *Phys. Lett. B* **716** (2012) 30 [[1207.7235](#)].
- [3] ATLAS, CMS collaboration, *Combined Measurement of the Higgs Boson Mass in pp Collisions at $\sqrt{s} = 7$ and 8 TeV with the ATLAS and CMS Experiments*, *Phys. Rev. Lett.* **114** (2015) 191803 [[1503.07589](#)].
- [4] BABAR collaboration, *Evidence for an excess of $\bar{B} \rightarrow D^{(*)}\tau^-\bar{\nu}_\tau$ decays*, *Phys. Rev. Lett.* **109** (2012) 101802 [[1205.5442](#)].
- [5] BABAR collaboration, *Measurement of an Excess of $\bar{B} \rightarrow D^{(*)}\tau^-\bar{\nu}_\tau$ Decays and Implications for Charged Higgs Bosons*, *Phys. Rev. D* **88** (2013) 072012 [[1303.0571](#)].
- [6] LHCb collaboration, *Measurement of the ratio of branching fractions $\mathcal{B}(\bar{B}^0 \rightarrow D^{*+}\tau^-\bar{\nu}_\tau)/\mathcal{B}(\bar{B}^0 \rightarrow D^{*+}\mu^-\bar{\nu}_\mu)$* , *Phys. Rev. Lett.* **115** (2015) 111803 [[1506.08614](#)].
- [7] BELLE collaboration, *Measurement of the branching ratio of $\bar{B} \rightarrow D^{(*)}\tau^-\bar{\nu}_\tau$ relative to $\bar{B} \rightarrow D^{(*)}\ell^-\bar{\nu}_\ell$ decays with hadronic tagging at Belle*, *Phys. Rev. D* **92** (2015) 072014 [[1507.03233](#)].
- [8] BELLE collaboration, *Measurement of the τ lepton polarization and $R(D^*)$ in the decay $\bar{B} \rightarrow D^*\tau^-\bar{\nu}_\tau$* , *Phys. Rev. Lett.* **118** (2017) 211801 [[1612.00529](#)].
- [9] LHCb collaboration, *Measurement of the ratio of the $B^0 \rightarrow D^{*-}\tau^+\nu_\tau$ and $B^0 \rightarrow D^{*-}\mu^+\nu_\mu$ branching fractions using three-prong τ -lepton decays*, *Phys. Rev. Lett.* **120** (2018) 171802 [[1708.08856](#)].
- [10] BELLE collaboration, *Measurement of the τ lepton polarization and $R(D^*)$ in the decay $\bar{B} \rightarrow D^*\tau^-\bar{\nu}_\tau$ with one-prong hadronic τ decays at Belle*, *Phys. Rev. D* **97** (2018) 012004 [[1709.00129](#)].
- [11] LHCb collaboration, *Test of Lepton Flavor Universality by the measurement of the $B^0 \rightarrow D^{*-}\tau^+\nu_\tau$ branching fraction using three-prong τ decays*, *Phys. Rev. D* **97** (2018) 072013 [[1711.02505](#)].
- [12] BELLE collaboration, *Measurement of $\mathcal{R}(D)$ and $\mathcal{R}(D^*)$ with a semileptonic tagging method*, *Phys. Rev. Lett.* **124** (2020) 161803 [[1910.05864](#)].
- [13] HFLAV collaboration, *Averages of b-hadron, c-hadron, and τ -lepton properties as of 2018*, [1909.12524](#).
- [14] HFLAV collaboration, *Online update for averages of R_D and R_{D^*} for Spring 2019 at <https://hflav-eos.web.cern.ch/hflav-eos/semi/spring19/html/RDsDsstar/RDRDs.html>*, .
- [15] M. Bordone, M. Jung and D. van Dyk, *Theory determination of $\bar{B} \rightarrow D^{(*)}\ell^-\bar{\nu}$ form factors at $\mathcal{O}(1/m_c^2)$* , *Eur. Phys. J. C* **80** (2020) 74 [[1908.09398](#)].
- [16] A.K. Alok, D. Kumar, J. Kumar, S. Kumbhakar and S.U. Sankar, *New physics solutions for R_D and R_{D^*}* , *JHEP* **09** (2018) 152 [[1710.04127](#)].
- [17] Q.-Y. Hu, X.-Q. Li and Y.-D. Yang, *$b \rightarrow c\tau\nu$ transitions in the standard model effective field theory*, *Eur. Phys. J. C* **79** (2019) 264 [[1810.04939](#)].
- [18] A.K. Alok, D. Kumar, S. Kumbhakar and S. Uma Sankar, *Solutions to R_D - R_{D^*} in light of Belle 2019 data*, *Nucl. Phys. B* **953** (2020) 114957 [[1903.10486](#)].
- [19] C. Murgui, A. Peñuelas, M. Jung and A. Pich, *Global fit to $b \rightarrow c\tau\nu$ transitions*, *JHEP* **09** (2019) 103 [[1904.09311](#)].

- [20] M. Blanke, A. Crivellin, S. de Boer, T. Kitahara, M. Moscati, U. Nierste et al., *Impact of polarization observables and $B_c \rightarrow \tau\nu$ on new physics explanations of the $b \rightarrow c\tau\nu$ anomaly*, *Phys. Rev. D* **99** (2019) 075006 [[1811.09603](#)].
- [21] M. Blanke, A. Crivellin, T. Kitahara, M. Moscati, U. Nierste and I. Nišandžić, *Addendum to “Impact of polarization observables and $B_c \rightarrow \tau\nu$ on new physics explanations of the $b \rightarrow c\tau\nu$ anomaly”*, [1905.08253](#).
- [22] K. Cheung, Z.-R. Huang, H.-D. Li, C.-D. Lü, Y.-N. Mao and R.-Y. Tang, *Revisit to the $b \rightarrow c\tau\nu$ transition: In and beyond the SM*, *Nucl. Phys. B* **965** (2021) 115354 [[2002.07272](#)].
- [23] S. Kumbhakar, *Signatures of complex new physics in $b \rightarrow c\tau\bar{\nu}$ transitions*, *Nucl. Phys. B* **963** (2021) 115297 [[2007.08132](#)].
- [24] M. Tanaka and R. Watanabe, *New physics in the weak interaction of $\bar{B} \rightarrow D^{(*)}\tau\bar{\nu}$* , *Phys. Rev. D* **87** (2013) 034028 [[1212.1878](#)].
- [25] Y. Sakaki, M. Tanaka, A. Tayduganov and R. Watanabe, *Testing leptoquark models in $\bar{B} \rightarrow D^{(*)}\tau\bar{\nu}$* , *Phys. Rev. D* **88** (2013) 094012 [[1309.0301](#)].
- [26] M. Bauer and M. Neubert, *Minimal Leptoquark Explanation for the $R_{D^{(*)}}$, R_K , and $(g-2)_g$ Anomalies*, *Phys. Rev. Lett.* **116** (2016) 141802 [[1511.01900](#)].
- [27] S. Fajfer and N. Košnik, *Vector leptoquark resolution of R_K and $R_{D^{(*)}}$ puzzles*, *Phys. Lett. B* **755** (2016) 270 [[1511.06024](#)].
- [28] X.-Q. Li, Y.-D. Yang and X. Zhang, *Revisiting the one leptoquark solution to the $R(D^{(*)})$ anomalies and its phenomenological implications*, *JHEP* **08** (2016) 054 [[1605.09308](#)].
- [29] A. Crivellin, D. Müller and T. Ota, *Simultaneous explanation of $R(D^{(*)})$ and $b \rightarrow s\mu^+\mu^-$: the last scalar leptoquarks standing*, *JHEP* **09** (2017) 040 [[1703.09226](#)].
- [30] D. Bečirević, I. Doršner, S. Fajfer, N. Košnik, D.A. Faroughy and O. Sumensari, *Scalar leptoquarks from grand unified theories to accommodate the B -physics anomalies*, *Phys. Rev. D* **98** (2018) 055003 [[1806.05689](#)].
- [31] A. Angelescu, D. Bečirević, D. Faroughy and O. Sumensari, *Closing the window on single leptoquark solutions to the B -physics anomalies*, *JHEP* **10** (2018) 183 [[1808.08179](#)].
- [32] S. Bansal, R.M. Capdevilla and C. Kolda, *Constraining the minimal flavor violating leptoquark explanation of the $R_{D^{(*)}}$ anomaly*, *Phys. Rev. D* **99** (2019) 035047 [[1810.11588](#)].
- [33] S. Iguro, T. Kitahara, Y. Omura, R. Watanabe and K. Yamamoto, *D^* polarization vs. $R_{D^{(*)}}$ anomalies in the leptoquark models*, *JHEP* **02** (2019) 194 [[1811.08899](#)].
- [34] A. Crivellin, D. Müller and F. Saturnino, *Flavor Phenomenology of the Leptoquark Singlet-Triplet Model*, *JHEP* **06** (2020) 020 [[1912.04224](#)].
- [35] N. Deshpande and X.-G. He, *Consequences of R -parity violating interactions for anomalies in $\bar{B} \rightarrow D^{(*)}\tau\bar{\nu}$ and $b \rightarrow s\mu^+\mu^-$* , *Eur. Phys. J. C* **77** (2017) 134 [[1608.04817](#)].
- [36] W. Altmannshofer, P. Bhupal Dev and A. Soni, *$R_{D^{(*)}}$ anomaly: A possible hint for natural supersymmetry with R -parity violation*, *Phys. Rev. D* **96** (2017) 095010 [[1704.06659](#)].
- [37] Q.-Y. Hu, X.-Q. Li, Y. Muramatsu and Y.-D. Yang, *R -parity violating solutions to the $R_{D^{(*)}}$ anomaly and their GUT-scale unifications*, *Phys. Rev. D* **99** (2019) 015008 [[1808.01419](#)].
- [38] Q.-Y. Hu, Y.-D. Yang and M.-D. Zheng, *Revisiting the B -physics anomalies in R -parity violating MSSM*, *Eur. Phys. J. C* **80** (2020) 365 [[2002.09875](#)].

- [39] W. Altmannshofer, P.B. Dev, A. Soni and Y. Sui, *Addressing $R_{D^{(*)}}$, $R_{K^{(*)}}$, muon $g - 2$ and ANITA anomalies in a minimal R -parity violating supersymmetric framework*, *Phys. Rev. D* **102** (2020) 015031 [2002.12910].
- [40] A. Crivellin, C. Greub and A. Kokulu, *Explaining $B \rightarrow D\tau\nu$, $B \rightarrow D^*\tau\nu$ and $B \rightarrow \tau\nu$ in a 2HDM of type III*, *Phys. Rev. D* **86** (2012) 054014 [1206.2634].
- [41] A. Celis, M. Jung, X.-Q. Li and A. Pich, *Sensitivity to charged scalars in $B \rightarrow D^{(*)}\tau\nu_\tau$ and $B \rightarrow \tau\nu_\tau$ decays*, *JHEP* **01** (2013) 054 [1210.8443].
- [42] P. Ko, Y. Omura and C. Yu, *$B \rightarrow D^{(*)}\tau\nu$ and $B \rightarrow \tau\nu$ in chiral $U(1)'$ models with flavored multi Higgs doublets*, *JHEP* **03** (2013) 151 [1212.4607].
- [43] A. Celis, M. Jung, X.-Q. Li and A. Pich, *Scalar contributions to $b \rightarrow c(u)\tau\nu$ transitions*, *Phys. Lett. B* **771** (2017) 168 [1612.07757].
- [44] P. Asadi, M.R. Buckley and D. Shih, *It's all right(-handed neutrinos): a new W' model for the $R_{D^{(*)}}$ anomaly*, *JHEP* **09** (2018) 010 [1804.04135].
- [45] A. Greljo, D.J. Robinson, B. Shakya and J. Zupan, *$R(D^{(*)})$ from W' and right-handed neutrinos*, *JHEP* **09** (2018) 169 [1804.04642].
- [46] K. Babu, B. Dutta and R.N. Mohapatra, *A theory of $R(D^*, D)$ anomaly with right-handed currents*, *JHEP* **01** (2019) 168 [1811.04496].
- [47] M. Blanke and A. Crivellin, *B Meson Anomalies in a Pati-Salam Model within the Randall-Sundrum Background*, *Phys. Rev. Lett.* **121** (2018) 011801 [1801.07256].
- [48] LHCb collaboration, *Measurement of the ratio of branching fractions $\mathcal{B}(B_c^+ \rightarrow J/\psi\tau^+\nu_\tau)/\mathcal{B}(B_c^+ \rightarrow J/\psi\mu^+\nu_\mu)$* , *Phys. Rev. Lett.* **120** (2018) 121801 [1711.05623].
- [49] LATTICE-HPQCD collaboration, *$R(J/\psi)$ and $B_c^- \rightarrow J/\psi\ell^-\bar{\nu}_\ell$ Lepton Flavor Universality Violating Observables from Lattice QCD*, *Phys. Rev. Lett.* **125** (2020) 222003 [2007.06956].
- [50] HPQCD collaboration, *$B_c \rightarrow J/\psi$ form factors for the full q^2 range from lattice QCD*, *Phys. Rev. D* **102** (2020) 094518 [2007.06957].
- [51] R. Watanabe, *New Physics effect on $B_c \rightarrow J/\psi\tau\bar{\nu}$ in relation to the $R_{D^{(*)}}$ anomaly*, *Phys. Lett. B* **776** (2018) 5 [1709.08644].
- [52] J. Zhu, B. Wei, J.-H. Sheng, R.-M. Wang, Y. Gao and G.-R. Lu, *Probing the R -parity violating supersymmetric effects in $B_c \rightarrow J/\psi\ell^-\bar{\nu}_\ell$, $\eta_c\ell^-\bar{\nu}_\ell$ and $\Lambda_b \rightarrow \Lambda_c\ell^-\bar{\nu}_\ell$ decays*, *Nucl. Phys. B* **934** (2018) 380 [1801.00917].
- [53] C.-T. Tran, M.A. Ivanov, J.G. Körner and P. Santorelli, *Implications of new physics in the decays $B_c \rightarrow (J/\psi, \eta_c)\tau\nu$* , *Phys. Rev. D* **97** (2018) 054014 [1801.06927].
- [54] A. Issadykov and M.A. Ivanov, *The decays $B_c \rightarrow J/\psi + \bar{\ell}\nu_\ell$ and $B_c \rightarrow J/\psi + \pi(K)$ in covariant confined quark model*, *Phys. Lett. B* **783** (2018) 178 [1804.00472].
- [55] T.D. Cohen, H. Lamm and R.F. Lebed, *Tests of the standard model in $B \rightarrow D\ell\nu_\ell$, $B \rightarrow D^*\ell\nu_\ell$ and $B_c \rightarrow J/\psi\ell\nu_\ell$* , *Phys. Rev. D* **98** (2018) 034022 [1807.00256].
- [56] T.D. Cohen, H. Lamm and R.F. Lebed, *Model-independent bounds on $R(J/\psi)$* , *JHEP* **09** (2018) 168 [1807.02730].
- [57] Z.-R. Huang, Y. Li, C.-D. Lu, M.A. Paracha and C. Wang, *Footprints of New Physics in $b \rightarrow c\tau\nu$ Transitions*, *Phys. Rev. D* **98** (2018) 095018 [1808.03565].

- [58] W. Wang and R. Zhu, *Model independent investigation of the $R_{J/\psi, \eta_c}$ and ratios of decay widths of semileptonic B_c decays into a P-wave charmonium*, *Int. J. Mod. Phys. A* **34** (2019) 1950195 [1808.10830].
- [59] D. Lejnak, B. Melic and M. Patra, *On lepton flavour universality in semileptonic $B_c \rightarrow \eta_c, J/\psi$ decays*, *JHEP* **05** (2019) 094 [1901.08368].
- [60] X.-Q. Hu, S.-P. Jin and Z.-J. Xiao, *Semileptonic decays $B_c \rightarrow (\eta_c, J/\psi)l\bar{\nu}_l$ in the "PQCD + Lattice" approach*, *Chin. Phys. C* **44** (2020) 023104 [1904.07530].
- [61] N. Penalva, E. Hernández and J. Nieves, *$\bar{B}_c \rightarrow \eta_c, \bar{B}_c \rightarrow J/\psi$ and $\bar{B} \rightarrow D^{(*)}$ semileptonic decays including new physics*, *Phys. Rev. D* **102** (2020) 096016 [2007.12590].
- [62] A. Berns and H. Lamm, *Model-Independent Prediction of $R(\eta_c)$* , *JHEP* **12** (2018) 114 [1808.07360].
- [63] C.W. Murphy and A. Soni, *Model-Independent Determination of $B_c^+ \rightarrow \eta_c \ell^+ \nu$ Form Factors*, *Phys. Rev. D* **98** (2018) 094026 [1808.05932].
- [64] R. Dutta, *$\Lambda_b \rightarrow (\Lambda_c, p) \tau \nu$ decays within standard model and beyond*, *Phys. Rev. D* **93** (2016) 054003 [1512.04034].
- [65] X.-Q. Li, Y.-D. Yang and X. Zhang, *$\Lambda_b \rightarrow \Lambda_c \tau \bar{\nu}_\tau$ decay in scalar and vector leptoquark scenarios*, *JHEP* **02** (2017) 068 [1611.01635].
- [66] E. Di Salvo, F. Fontanelli and Z. Ajaltouni, *Detailed Study of the Decay $\Lambda_b \rightarrow \Lambda_c \tau \bar{\nu}_\tau$* , *Int. J. Mod. Phys. A* **33** (2018) 1850169 [1804.05592].
- [67] A. Ray, S. Sahoo and R. Mohanta, *Probing new physics in semileptonic Λ_b decays*, *Phys. Rev. D* **99** (2019) 015015 [1812.08314].
- [68] N. Penalva, E. Hernández and J. Nieves, *Further tests of lepton flavour universality from the charged lepton energy distribution in $b \rightarrow c$ semileptonic decays: The case of $\Lambda_b \rightarrow \Lambda_c \ell \bar{\nu}_\ell$* , *Phys. Rev. D* **100** (2019) 113007 [1908.02328].
- [69] X.-L. Mu, Y. Li, Z.-T. Zou and B. Zhu, *Investigation of effects of new physics in $\Lambda_b \rightarrow \Lambda_c \tau \bar{\nu}_\tau$ decay*, *Phys. Rev. D* **100** (2019) 113004 [1909.10769].
- [70] T. Gutsche, M.A. Ivanov, J.G. Körner, V.E. Lyubovitskij, P. Santorelli and N. Haby1, *Semileptonic decay $\Lambda_b \rightarrow \Lambda_c + \tau^- + \bar{\nu}_\tau$ in the covariant confined quark model*, *Phys. Rev. D* **91** (2015) 074001 [1502.04864].
- [71] S. Shivashankara, W. Wu and A. Datta, *$\Lambda_b \rightarrow \Lambda_c \tau \bar{\nu}_\tau$ Decay in the Standard Model and with New Physics*, *Phys. Rev. D* **91** (2015) 115003 [1502.07230].
- [72] P. Böer, A. Kokulu, J.-N. Toelstede and D. van Dyk, *Angular Analysis of $\Lambda_b \rightarrow \Lambda_c(\rightarrow \Lambda \pi) \ell \bar{\nu}$* , *JHEP* **12** (2019) 082 [1907.12554].
- [73] M. Ferrillo, A. Mathad, P. Owen and N. Serra, *Probing effects of new physics in $\Lambda_b^0 \rightarrow \Lambda_c^+ \mu^- \bar{\nu}_\mu$ decays*, *JHEP* **12** (2019) 148 [1909.04608].
- [74] Q.-Y. Hu, X.-Q. Li, Y.-D. Yang and D.-H. Zheng, *The measurable angular distribution of $\Lambda_b^0 \rightarrow \Lambda_c^+ (\rightarrow \Lambda^0 \pi^+) \tau^- (\rightarrow \pi^- \nu_\tau) \bar{\nu}_\tau$ decay*, *JHEP* **02** (2021) 183 [2011.05912].
- [75] R. Dutta, *Phenomenology of $\Xi_b \rightarrow \Xi_c \tau \nu$ decays*, *Phys. Rev. D* **97** (2018) 073004 [1801.02007].
- [76] R. Faustov and V. Galkin, *Relativistic description of the Ξ_b baryon semileptonic decays*, *Phys. Rev. D* **98** (2018) 093006 [1810.03388].

- [77] J. Zhang, J. Su and Q. Zeng, *Contributions of vector leptoquark to $\Xi_b \rightarrow \Xi_c \tau \bar{\nu}_\tau$ decay*, *Nucl. Phys. B* **938** (2019) 131.
- [78] J. Zhang, X. An, R. Sun and J. Su, *Probing new physics in semileptonic $\Xi_b \rightarrow \Lambda(\Xi_c) \tau^- \bar{\nu}_\tau$ decays*, *Eur. Phys. J. C* **79** (2019) 863.
- [79] N. Rajeev, R. Dutta and S. Kumbhakar, *Implication of $R_{D^{(*)}}$ anomalies on semileptonic decays of Σ_b and Ω_b baryons*, *Phys. Rev. D* **100** (2019) 035015 [[1905.13468](#)].
- [80] J.-H. Sheng, J. Zhu, X.-N. Li, Q.-Y. Hu and R.-M. Wang, *Probing new physics in semileptonic Σ_b and Ω_b decays*, *Phys. Rev. D* **102** (2020) 055023 [[2009.09594](#)].
- [81] V.V. Kiselev, A.K. Likhoded and A.I. Onishchenko, *Semileptonic B_c meson decays in sum rules of QCD and NRQCD*, *Nucl. Phys.* **B569** (2000) 473 [[hep-ph/9905359](#)].
- [82] M.A. Ivanov, J.G. Korner and P. Santorelli, *The Semileptonic decays of the B_c meson*, *Phys. Rev.* **D63** (2001) 074010 [[hep-ph/0007169](#)].
- [83] D. Ebert, R.N. Faustov and V.O. Galkin, *Weak decays of the B_c meson to charmonium and D mesons in the relativistic quark model*, *Phys. Rev.* **D68** (2003) 094020 [[hep-ph/0306306](#)].
- [84] E. Hernandez, J. Nieves and J.M. Verde-Velasco, *Study of exclusive semileptonic and non-leptonic decays of B_c - in a nonrelativistic quark model*, *Phys. Rev.* **D74** (2006) 074008 [[hep-ph/0607150](#)].
- [85] M.A. Ivanov, J.G. Körner and P. Santorelli, *Exclusive semileptonic and nonleptonic decays of the B_c meson*, *Phys. Rev.* **D73** (2006) 054024 [[hep-ph/0602050](#)].
- [86] W. Wang, Y.-L. Shen and C.-D. Lu, *Covariant Light-Front Approach for B_c transition form factors*, *Phys. Rev.* **D79** (2009) 054012 [[0811.3748](#)].
- [87] C.-F. Qiao and R.-L. Zhu, *Estimation of semileptonic decays of B_c meson to S -wave charmonia with nonrelativistic QCD*, *Phys. Rev.* **D87** (2013) 014009 [[1208.5916](#)].
- [88] W.-F. Wang, Y.-Y. Fan and Z.-J. Xiao, *Semileptonic decays $B_c \rightarrow (\eta_c, J/\Psi) l \nu$ in the perturbative QCD approach*, *Chin. Phys.* **C37** (2013) 093102 [[1212.5903](#)].
- [89] Z. Rui, H. Li, G.-x. Wang and Y. Xiao, *Semileptonic decays of B_c meson to S -wave charmonium states in the perturbative QCD approach*, *Eur. Phys. J.* **C76** (2016) 564 [[1602.08918](#)].
- [90] R. Dutta and A. Bhol, *$B_c \rightarrow (J/\psi, \eta_c) \tau \nu$ semileptonic decays within the standard model and beyond*, *Phys. Rev.* **D96** (2017) 076001 [[1701.08598](#)].
- [91] HPQCD collaboration, *B_c decays from highly improved staggered quarks and NRQCD*, *PoS LATTICE2016* (2016) 281 [[1611.01987](#)].
- [92] A. Lytle, B. Colquhoun, C. Davies, J. Koponen and C. McNeile, *Semileptonic B_c decays from full lattice QCD*, *PoS BEAUTY2016* (2016) 069 [[1605.05645](#)].
- [93] B. Bhattacharya, A. Datta, S. Kamali and D. London, *A measurable angular distribution for $\bar{B} \rightarrow D^* \tau^- \bar{\nu}_\tau$ decays*, *JHEP* **07** (2020) 194 [[2005.03032](#)].
- [94] R. Dutta, A. Bhol and A.K. Giri, *Effective theory approach to new physics in $b \rightarrow u$ and $b \rightarrow c$ leptonic and semileptonic decays*, *Phys. Rev. D* **88** (2013) 114023 [[1307.6653](#)].
- [95] Z. Ligeti, M. Papucci and D.J. Robinson, *New Physics in the Visible Final States of $B \rightarrow D^{(*)} \tau \nu$* , *JHEP* **01** (2017) 083 [[1610.02045](#)].

- [96] R. Mandal, C. Murgui, A. Peñuelas and A. Pich, *The role of right-handed neutrinos in $b \rightarrow c\tau\bar{\nu}$ anomalies*, *JHEP* **08** (2020) 022 [[2004.06726](#)].
- [97] M. Beneke and T. Feldmann, *Symmetry breaking corrections to heavy to light B meson form-factors at large recoil*, *Nucl. Phys. B* **592** (2001) 3 [[hep-ph/0008255](#)].
- [98] R. Alonso, B. Grinstein and J. Martin Camalich, *Lifetime of B_c^- Constrains Explanations for Anomalies in $B \rightarrow D^{(*)}\tau\nu$* , *Phys. Rev. Lett.* **118** (2017) 081802 [[1611.06676](#)].
- [99] D. Bečirević, M. Fedele, I. Nišandžić and A. Tayduganov, *Lepton Flavor Universality tests through angular observables of $\bar{B} \rightarrow D^{(*)}\ell\bar{\nu}$ decay modes*, [1907.02257](#).
- [100] P. Asadi, A. Hallin, J. Martin Camalich, D. Shih and S. Westhoff, *Complete framework for tau polarimetry in $B \rightarrow D^{(*)}\tau\nu$ decays*, *Phys. Rev. D* **102** (2020) 095028 [[2006.16416](#)].
- [101] M. Algueró, S. Descotes-Genon, J. Matias and M. Novoa-Brunet, *Symmetries in $B \rightarrow D^*\ell\nu$ angular observables*, *JHEP* **06** (2020) 156 [[2003.02533](#)].
- [102] U. Egede, T. Hurth, J. Matias, M. Ramon and W. Reece, *New physics reach of the decay mode $\bar{B} \rightarrow \bar{K}^{*0}\ell^+\ell^-$* , *JHEP* **10** (2010) 056 [[1005.0571](#)].
- [103] J. Matias, F. Mescia, M. Ramon and J. Virto, *Complete Anatomy of $\bar{B}_d \rightarrow \bar{K}^{*0}(\rightarrow K\pi)l^+l^-$ and its angular distribution*, *JHEP* **04** (2012) 104 [[1202.4266](#)].
- [104] L. Hofer and J. Matias, *Exploiting the symmetries of P and S wave for $B \rightarrow K^*\mu^+\mu^-$* , *JHEP* **09** (2015) 104 [[1502.00920](#)].
- [105] P. Auvil and J. Brehm, *Wave Functions for Particles of Higher Spin*, *Phys. Rev.* **145** (1966) 1152.
- [106] H.E. Haber, *Spin formalism and applications to new physics searches*, in *21st Annual SLAC Summer Institute on Particle Physics: Spin Structure in High-energy Processes (School: 26 Jul - 3 Aug, Topical Conference: 4-6 Aug) (SSI 93)*, pp. 231–272, 4, 1994 [[hep-ph/9405376](#)].
- [107] M. Jacob and G.C. Wick, *On the General Theory of Collisions for Particles with Spin*, *Annals Phys.* **7** (1959) 404.